First posted online on 30 October 2017 as 10.1242/dev.152504
Access the most recent version at http://dev.biologists.org/lookup/doi/10.1242/dev.152504

Long noncoding RNA *ROCR* contributes to SOX9 expression and chondrogenic differentiation of human mesenchymal stem cells

Matt J. Barter[1], Rodolfo Gomez[2], Sam Hyatt[3], Kat Cheung[1], Andrew Skelton[1], Yaobo Xu[1], Ian Clark[4], David A. Young[1]

[1] Institute of Genetic Medicine, Newcastle University, Newcastle upon Tyne, NE1 3BZ, UK.

[2] Musculoskeletal Pathology Group, Institute IDIS, Travesia choupana s/n, Hospital Clínico Universitario de Santiago, Santiago de Compostela, 15706, Spain.

[3] Institute of Cancer and Genetics, School of Medicine, Cardiff University, Heath Park, Cardiff, CF14 4XN, United Kingdom.

[4] School of Biological Sciences, University of East Anglia, Norwich, United Kingdom.

Address correspondence to: David A. Young, PhD; Institute of Genetic Medicine, International Centre for Life, Newcastle University, Newcastle upon Tyne, NE1 3BZ, UK Tel +44 191 241 8831; E-mail: d.a.young@ncl.ac.uk

Summary statement

We identified a chondrocyte repertoire of lncRNAs and discovered that *ROCR* (regulator of chondrogenesis RNA) is important for MSC chondrogenesis and cartilage gene expression by promoting the expression of SOX9.

Abstract

Long non-coding RNAs (lncRNAs) are expressed in a highly tissue-specific manner where they function in various aspects of cell biology, often as key regulators of gene expression. In this study we established a role for lncRNAs in chondrocyte differentiation. Using RNA sequencing we identified a human articular chondrocyte repertoire of lncRNAs from normal hip cartilage donated by neck of femur fracture patients. Of particular interest are lncRNAs upstream of the master chondrocyte transcription factor SOX9 locus. SOX9 is an HMG-box transcription factor which is essential for chondrocyte development by directing the expression of chondrocyte specific genes. Two of these lncRNAs are upregulated during chondrogenic differentiation of MSCs. Depletion of one of these lncRNA, *LOC102723505*, which we termed *ROCR* (regulator of chondrogenesis RNA), by RNAi disrupted MSC chondrogenesis, concomitant with reduced cartilage-specific gene expression and incomplete matrix component production, indicating an important role in chondrocyte biology. Specifically, SOX9 induction was significantly ablated in the absence of *ROCR*, and overexpression of SOX9 rescued the differentiation of MSCs into chondrocytes. Our work sheds further light on chondrocyte specific SOX9 expression and highlights a novel method of chondrocyte gene regulation involving a lncRNA.

Key words: SOX9, lncRNA, cartilage, chondrogenesis, MSC, epigenetics, differentiation.

Introduction

Tens of thousands of long noncoding RNAs (lncRNAs) have been identified in the human genome through the use of RNA deep sequencing (RNA-Seq) (Iyer *et al.*, 2015). lncRNAs are classified as >200nt RNAs that derive from both intergenic and overlapping protein-coding gene regions (Derrien *et al.*, 2012). Detailed studies are beginning to ascribe functional roles for many of these lncRNAs, which appear to regulate numerous cell processes (Rinn and Chang, 2012). Indeed, lncRNAs have emerged as key regulators of gene expression transcriptionally and post-transcriptionally, acting through diverse mechanisms such as the regulation of epigenetic modifications and by acting as scaffolds for protein complex formation at gene loci (Rinn and Chang, 2012). lncRNAs display more tissue-specific expression patterns than protein coding genes and cell differentiation during development is particularly susceptible to experimental loss of lncRNAs (Derrien *et al.*, 2012; Sauvageau *et al.*, 2013; Fatica and Bozzoni, 2014). For example, lncRNAs play important roles in guiding limb development. In limb patterning HOTTIP is required for specification of mesenchyme condensation sites through promotion of HOXA gene expression by a cis-regulatory mechanism, and HOTAIR is now also recognised for a similar trans-acting role in regulating HOXD gene expression during skeletal patterning (Wang *et al.*, 2011; Li *et al.*, 2013).

Little is known about the expression of lncRNAs in cartilage or in the development of the chondrocyte, the sole cartilage cell type. Chondrocytes develop from condensations of mesenchymal cells in a process known as chondrogenesis, which is essential for development of the endochondral skeleton (Onyekwelu *et al.*, 2009). During chondrogenesis cells of the mesenchyme commit to a chondrocyte differentiation program then progress through multiple stages to specify the resting, proliferating and hypertrophic regions of the growth plate. They also constitute the articular cartilage at the ends of the long bones. This differentiation is a coordinated process determined by temporal and spatial expression of multiple growth factors and dependent on the specific activity of the HMG-box transcription factor SOX9 (Akiyama, 2008). SOX9 controls the expression of numerous chondrocyte genes including its co-factors L-SOX5a and SOX6, and extracellular matrix genes such as type II collagen and the proteoglycan aggrecan. Experimental loss of SOX9 abrogates limb development in mice (Akiyama, 2008; Akiyama and Lefebvre, 2011) and mutations in the *SOX9* coding sequence lead to the skeletal malformation syndrome campomelic dysplasia (CD) (Foster *et al.*, 1994; Wagner *et al.*, 1994). DNA alterations around the *SOX9* locus can also lead to CD, highlighting the complex regulatory mechanisms governing *SOX9* expression (Foster *et al.*, 1994; Wagner *et al.*, 1994).

SOX9 is found in a gene desert on chromosome 17, as is common for developmental transcription factors, surrounded by many potential regulatory regions. However, the cellular mechanisms for regulating *SOX9* are not fully established. Analyses of campomelic dysplasia patient chromosomal rearrangements and promoter YAC transgenes suggest certain chondrogenesis-specific enhancers lie in a region between 50kb and 350kb upstream of *SOX9* (Foster *et al.*, 1994; Wagner *et al.*, 1994; Wunderle *et al.*, 1998; Gordon *et al.*, 2009). SOX9 also specifies the fate of other lineages, including Sertoli cells, neural stem cells, pancreas progenitor cells and neural crest, neuronal, glial, heart valve, gut and kidney cells (Pritchett *et al.*, 2011). Again tissue specific enhancers have been demonstrated to regulate the expression in some of these tissues (Gordon *et al.*, 2009).

cDNA cloning methods and *in silico* genome analysis have established that numerous ESTs and predicted transcripts are localised to these enhancer regions upstream of *SOX9* but it is unclear which are expressed in particular tissues and whether any have a functional role in chondrocytes. We established a chondrocyte repertoire of lncRNAs and confirmed the presence of a number of transcripts around the *SOX9* locus with whole transcriptome analysis of human articular cartilage RNA by RNA-Seq. We discovered a novel cartilage specific 4 exon lncRNA corresponding to a 3 exon RefSeq transcript *LOC102723505* (Ensembl transcript *ENST00000430908*) 94kb upstream of *SOX9*, which we termed *ROCR* (Regulator of Chondrogenesis RNA). This lncRNA is required for successful differentiation of mesenchymal stem cells (MSCs) into chondrocytes where it appears to contribute to *SOX9* expression. Thus, we have identified a previously unknown mechanism of *SOX9* regulation involving a chondrocyte-specific lncRNA.

Results

RNA-Seq was performed on normal human hip articular chondrocyte RNA obtained from female neck of femur (NOF) fracture patients to establish the adult chondrocyte transcriptome and its complement of lncRNAs (6 samples; median age=76 years). Of the 46,087 transcripts identified (FPKM>1) 813 were annotated as lncRNAs (Supp. Table 2). Examination of cartilage RNA-Seq reads uploaded to the UCSC genome browser identified processed transcripts upstream of the *SOX9* locus on chromosome 17, with robust expression of transcripts corresponding to *SOX9-AS1* and *LOC102723505* (Fig. 1A), exon/intron boundaries, and evidence of transcript start and end sites using CAGE (cap analysis gene expression) and PolyA-Seq data (Consortium, 2012; Flicek *et al.*, 2014) (Supp. Fig. 1). Proximal to the *SOX9* locus transcript variants of *SOX9-AS1* were detected partially corresponding to Refseq and

predicted Ensembl transcripts. 94kb upstream of *SOX9* we detected a novel 4 exon variant of an existing 3 exon RefSeq transcript *LOC102723505.* We designated 3 exon *LOC102723505* as *ROCR (regulator of chondrogenesis RNA)* transcript variant 1 and the novel 4 exon isoform *ROCR* transcript variant 2. We noted the presence of chromatin features of actively transcribed genes such as histone H3 lysine 4 trimethylation (H3K4me3) at the presumed *ROCR* promoter and enhancer-like signatures based on histone lysine 27 acetylation (H3K27ac) states from ENCODE chromatin state data (Fig. 1A, Supp. Fig. 1) (Ernst *et al.*, 2011). The *ROCR* locus is also notable for the expression of an additional lncRNA, *LINC01152*, albeit at very low levels in cartilage. In comparison with other coding transcripts *SOX9-AS1* and *ROCR* were robustly expressed in cartilage with FPKM (Fragments Per Kilobase Of Exon Per Million Fragments Mapped) in the range of 5-15, approximately 10% of the level of *SOX9* itself (Supp. Table 2).

We confirmed the expression of *SOX9-AS1* and *ROCR* in human articular cartilage by qRT-PCR with two assays per transcript targeted to different exons (Fig. 1B). The *ROCR* exon1-2 assay detects only transcript variant 2. Rapid amplification of cDNA ends (RACE) confirmed the presence of this novel 4 exon 574-base *ROCR* transcript (variant 2) in cartilage (Supp. Fig. 2). We are also able to identify this *ROCR* variant by subsequent analysis of RNA-Seq data from knee cartilage RNA (Dunn *et al.*, 2016). The majority of lncRNAs are considered to have nuclear functions and are often found enriched in the nucleus (Quinodoz and Guttman, 2014). In contrast to the nuclear enrichment of small nuclear RNA U2, we found both *SOX9-AS1* and *ROCR* were enriched in the cytoplasm, comparable with the localisation of the *SOX9* transcript itself (Fig. 1C). RNA-FISH analysis of *ROCR* in HAC was unsuccessful owing to the low expression and short transcript sequence limiting design of sufficient singly labelled Stellaris RNA-FISH probes (data not shown). In silico analysis indicates a lack of coding potential for both *SOX9-AS1* and *ROCR*, with the existence of only very short open reading frames (ORF Finder) and codon substitution rates indicative of noncoding transcripts (CPAT, CPC and PhyloCSF) (Supp. Fig. 3). *SOX9* is expressed in a variety of tissues but lncRNAs are reported to be more tissue specific (Derrien *et al.*, 2012). Accordingly we examined expression of *SOX9-AS1* and *ROCR* in additional joint tissues extracted from OA patients. *SOX9-AS1* was also expressed in synovium and fat pad tissue but *ROCR* was largely undetected and may thus be specific to cartilage in the joint (Fig. 1D).

We further examined transcript expression bioinformatically using publicly available cell and tissue RNA-Seq databases. Reads corresponding to *SOX9-AS1* were found in numerous cells types in both Human Protein Atlas (http://www.proteinatlas.org/) and Illumina BodyMap (ArrayExpress accession: E-MTAB-513; http://www.ebi.ac.uk/arrayexpress) sequence data (Supp. Table. 3) (Consortium, 2012; Krupp *et al.*, 2012; Fagerberg *et al.*, 2014; Flicek *et al.*, 2014). Reads corresponding to the 3 exons of

ROCR transcript variant 1 were found in pancreas and salivary gland tissue samples in the Human Protein Atlas RNA-Seq data and in breast tissue samples sequenced in the Illumina BodyMap data. Consistent with this analysis, further examination of expression by qRT-PCR across a 20-tissue RNA panel again identified the presence of *SOX9-AS1* transcripts in a number of tissues (Fig. 1E), albeit less than *SOX9* itself (Supp. Fig. 4). In contrast, detection of the novel *ROCR* transcript variant 2 was limited to chondrocytes alone (Fig. 1F), while the *ROCR* transcript variant 1 was additionally detected in brain and testis.

Considering the proximity of these transcripts to *SOX9* and the potential chondrocyte specificity of *ROCR* we sought to establish whether *SOX9-AS1* and *ROCR* were regulated during chondrocyte development. Accordingly we characterised expression of these lncRNAs using a robust transwell MSC chondrogenesis method which produces a uniform cartilage disc with rapid and substantial induction of chondrocyte gene expression, albeit including the expression of chondrocyte hypertrophy genes, thus differing from articular cartilage (Fig. 2A) (Murdoch *et al.*, 2007). *SOX9* expression is upregulated during chondrogenesis. Similarly, the expression of both *SOX9-AS1* and *ROCR* was induced during MSC chondrogenesis, paralleling the kinetics of *SOX9* expression (Fig. 2 B-C). In contrast, *LINC01152,* a potential testis specific lncRNA (D43770 Genbank ID), was downregulated during MSC chondrogenesis (Fig. 2D) (Ninomiya *et al.*, 1996). Interestingly, rapid amplification of cDNA ends (RACE) for MSC RNA identified a further 624-base isoform with an alternative first exon, which we termed *ROCR* transcript variant 3 (Supp. Fig. 1), situated in a bidirectional promoter locus with *LINC01152*.

MSC are capable of tri-lineage differentiation into chondrocytes, osteoblasts and adipocytes, dependent on specific differentiation factors (Pittenger *et al.*, 1999). We differentiated MSCs into osteoblasts and adipocytes by established methods and confirmed the expression of osteoblast specific markers alkaline phosphatase (*ALPL)* and *RUNX2*, and adipocyte specific genes adiponectin and *FABP* (Fig. 2E). *SOX9* was not upregulated during osteoblastogenesis or adipogenesis (Fig. 2F). Similarly, *SOX9-AS1* and *ROCR* were not upregulated during MSC osteoblastogenesis (Fig. 2G-H). *SOX9-AS1* was induced during MSC adipogenesis, in contrast to *ROCR*, but not to the level of chondrogenesis (Fig. 2G).

SOX9-AS1 and *ROCR* were both upregulated during chondrogenesis, with a profile similar to *SOX9*, thus we addressed their potential role during MSC chondrogenic differentiation by specific RNAi-mediated depletion (Fig. 3A). Reduction of *SOX9-AS1* expression had no effect on development of a cartilaginous disc (Fig. 3B and C). However, depletion of *ROCR* prevented disc formation (Fig. 3B) and caused a significant reduction in wet mass (Fig. 3C). Consistent with the disruption of disc formation following *ROCR* RNAi, matrix deposition in the form of glycosaminoglycan (GAG) polyanions was also

reduced (Fig. 3D). In case the transwell chondrogenesis method was particularly susceptible to experimental manipulation we also performed the traditional pellet chondrogenesis method and again found that *ROCR* was required for pellet development (Fig. 3E). Analysis of extracted sulphated GAG levels again indicated that *ROCR* is required for matrix GAG production (Fig. 3F). In addition, *ROCR* depletion reduced DNA levels suggesting it was required for the MSC proliferation during the early stages of chondrocyte differentiation (Fig. 3G) (Murdoch *et al.*, 2007).

Examination of chondrocyte gene expression following *SOX9-AS1* and *ROCR* RNAi indicated that depletion of *ROCR* also significantly abrogated the induction of cartilage ECM genes including *COL2A1* and *ACAN* (Fig. 4A). SOX9 is essential for cartilage matrix gene expression, so we assessed the impact of depletion of *SOX9-AS1* and *ROCR* at earlier timepoints in the chondrogenesis timecourse. Following *ROCR* depletion *SOX9* mRNA (Fig. 4B) and protein (Fig. 4C) was significantly reduced after 1 day of MSC differentiation and at even earlier time-points the upregulation of *SOX9* expression during MSC chondrogenesis was lost following *ROCR* depletion suggesting a critical role for *ROCR* in *SOX9* induction. During chondrogenesis SOX9 is required for expression of *SOX5* and *SOX6* which subsequently cooperate with SOX9 in directing chondrocyte gene expression (Akiyama *et al.*, 2002). *ROCR* depletion also prevented the upregulation of the SOX9 target genes *SOX5* and *SOX6*, which occured after *SOX9* induction (Fig. 4D).

To complement the role identified by RNAi for *ROCR* in MSC chondrogenesis and *SOX9* expression we also used an LNA GapmeR approach to deplete cellular *ROCR* levels (Supp. Fig. 5). Again the loss of *ROCR* resulted in a significant reduction in matrix GAG formation during MSC mini-pellet chondrogenesis with concomitant reduction in *SOX9* and matrix gene expression (Supp. Fig. 5). ROCR transcript variants 2 (HAC) and 3 (MSC) were cloned and overexpressed in MSCs and HAC by lentiviral transduction (Supp. Fig. 6). Overexpression of ROCR had no effect on SOX9 expression or induction of cartilage ECM genes COL2A1 and ACAN during MSC chondrogenesis (Supp. Fig. 6A). Overexpression of ROCR had no effect on SOX9 expression in HAC (Supp. Fig. 6B).

The above data suggested that *ROCR* is important for MSC chondrogenesis. We sought to establish whether the role of *ROCR* was specific to chondrocyte development consistent with its restricted expression profile. Accordingly we also performed *SOX9-AS1* and *ROCR* RNAi during MSC osteoblastogenesis and adipogenesis. Depletion of *ROCR* during osteoblast differentiation caused a partial decrease in matrix mineralisation (Fig. 5A and quantified in Fig. 5B), but no significant impact on *RUNX2* or *ALPL* expression (Fig. 5C). During MSC adipogenesis *ROCR* depletion had little effect, whereas *SOX9-AS1* depletion partially reduced fat droplet generation (Fig. 6D and quantified in Fig. 5E) and significantly decreased MSC adipogenic gene expression (Fig. 5F).

SOX9 is essential for chondrogenesis and since lncRNAs can contribute to the expression of neighbouring genes (Vance and Ponting, 2014) we reasoned the primary role of *ROCR* is to promote *SOX9* expression. Accordingly overexpression of SOX9 would be expected to rescue the chondrogenesis impairment caused by *ROCR* depletion. Lentiviral overexpression of SOX9 successfully enhanced MSC chondrogenesis (Fig. 6A-B). By overexpressing SOX9 and thereby returning the levels of SOX9 to those of control (Fig. 6C) the significant reduction of cartilage matrix GAG levels following depletion of *ROCR* was almost fully reversed (Fig. 6D). Reduction of *COL2A1* and *ACAN* by *ROCR* depletion was partially reversed by overexpression of SOX9 (Fig. 6E-F), while the levels of *L-SOX5a* and *SOX6* were completely rescued (Fig. 6G-H).

Discussion

In this study we established a panel of lncRNAs in normal human articular cartilage and identified two transcripts upstream of the *SOX9* locus that were upregulated during MSC chondrogenesis. One of these, *ROCR*, is a functional cartilage-restricted lncRNA which appeared important for chondrocyte differentiation where it may facilitate the induction of *SOX9* itself. This study established that a lncRNA contributes to SOX9 expression during differentiation of MSCs into chondrocytes thereby furthering our understanding of the key regulatory elements contained upstream of the *SOX9* promoter.

SOX9 is the master transcription factor governing chondrocyte development, as confirmed by genetic studies (Akiyama *et al.*, 2002). Regulation of SOX9 occurs at both the transcriptional and post-transcriptional level. Phosphorylation of SOX9 regulates its DNA binding activity and subcellular localisation, and numerous other interactions regulate SOX9 stability and facilitate its transcriptional activity (Kawakami *et al.*, 2006; Akiyama, 2008). At the transcriptional level induction of *SOX9* occurs rapidly during mesenchyme condensation in cartilage development both *in vivo* and *in vitro* (Wright *et al.*, 1995; Sekiya *et al.*, 2002), a process regulated by an interplay between growth factor signals and cell-cell interactions (Chimal-Monroy *et al.*, 2003; Yoon *et al.*, 2005). Our data indicated that during *in vitro* chondrogenesis a lncRNA, *ROCR*, is also important for this process.

A number of lncRNAs have key roles in stem cell differentiation, including *RMST* in neuronal differentiation, *Braveheart* in cardiac differentiation and *lnc-RAP1-10* in adipocyte differentiation (Klattenhoff *et al.*, 2013; Ng *et al.*, 2013; Perry and Ulitsky, 2016). Previously identified lncRNAs with a potential role in cartilage development include *DA125942* and *LncRNA-HIT* (Maass *et al.*, 2012; Carlson *et al.*, 2015). *DA125942*, a lncRNA transcribed from the *CISTR-ACT* locus interacts in cis with *PTHLH* and *trans* with *SOX9* to organise chromatin structure and promote transcription in cartilage

(Maass *et al.*, 2012). No direct role for the lncRNA in chondrogenesis was explored although the lncRNA locus was active during mouse limb bud development. *LncRNA-HIT*, expressed in mouse limb mesenchyme from the *Hoxa* gene locus, is able to bind and regulate DNA regions surrounding a number of cartilage genes including the *Hoxa* genes themselves (Carlson *et al.*, 2015). *LncRNA-HIT* may activate gene expression by binding to p100/CBP and it contributes to micromass chondrogenic differentiation of murine MSCs. Interestingly, we detected no RNA expression from the *CISTR-ACT* locus in our human cartilage RNA-Seq data and the conserved regions of *LncRNA-HIT* in human corresponded to an isoform of *HOXA13* with an extended 3'UTR rather than a lncRNA. It is possible these lncRNAs may be developmental stage or MSC specific. lncRNA *DANCR* may also promote chondrogenic differentiation of synovium-derived MSCs in concert with SOX4 (Zhang *et al.*, 2015). Two recent reviews elaborate on the roles of these lncRNAs during chondrogenesis (Huynh *et al.*, 2017; Lefebvre and Dvir-Ginzberg, 2017).

SOX9 is located in a ~2Mb gene desert on chromosome 17 in humans and lncRNA *ROCR* is expressed from a locus 94kb upstream of *SOX9*. Chromosomal rearrangements within this region are associated with campomelic dysplasia (CD), a skeletal malformation syndrome, and Pierre Robin sequence (PRS), a craniofacial disorder. Such disruptions can occur in regions up to and greater than 1Mb upstream of *SOX9* (Gordon *et al.*, 2009). Characterisation of these DNA alterations has indicated the presence of enhancer regions linked to the regulation of *SOX9* expression. Breakpoints causing more severe forms of CD are found more proximal to *SOX9* at locations 50-375kb upstream (Leipoldt *et al.*, 2007). Transgene and reporter experiments have also indicated that sequences in these locations are able to drive gene expression *in vivo* (Gordon *et al.*, 2009). More recent analysis confirmed the presence of a murine enhancer element at -70kb (-62kb in human) capable of regulating *SOX9* expression in a number of tissues (Mead *et al.*, 2013), and three further enhancers with prominent activity in chondrocytes at -84kb, -195kb and -250kb in mice (Yao *et al.*, 2015).

The *ROCR* locus sits within these enhancer regions and it is attractive to suggest that the lncRNA may contribute to the regulation of *SOX9 in vivo*. Indeed functional lncRNAs have been found to be enriched in genomic regions surrounding key developmental transcription factors (Orom *et al.*, 2010; Ulitsky *et al.*, 2011). In addition to skeletal malformations patients with CD often show XY sex reversal, with additional clinical features such as hearing loss, developmental delay, and occasional heart defects (Mansour *et al.*, 2002). Consistent with this, genetic ablation of *Sox9* in mice disrupts the differentiation of cells in the heart, central nervous system, testis, pancreas, gut and inner ear (Gordon *et al.*, 2009). Tissue specific enhancers regulate the expression of *SOX9*, for example the testis enhancer TES at -10kb, and our analysis suggested that *ROCR* is restricted to certain cell types:

cartilage, brain and testis, while *ROCR* variant 2 was only detected in cartilage. However our work focussed on RNA extracted from aged NOF and OA tissue and further work is required to confirm the expression of *ROCR* in normal healthy tissues. In combination with tissue specific enhancers *ROCR* may be required for the tightly coordinated spatio-temporal expression of *SOX9* during development. The expression level of *SOX9* in cartilage was 1-2 orders of magnitude higher than other tissues (Supp. Fig. 4) and we reasoned *ROCR* might also contribute to the magnitude of *SOX9* expression. But, in contrast to its role in chondrogenesis, we found no significant contribution by *ROCR* to *SOX9* expression levels in adult articular chondrocytes (Supp. Fig. 7A). The role of *ROCR* in *SOX9* expression might be in response to cues during chondrogenesis that are not present in cultured HAC and ROCR may additionally regulate other genes/proteins. The induction of both *SOX9-AS1* and *ROCR* paralleled the expression of *SOX9*. The activity of the aforementioned -70kb, -84kb and -195kb *SOX9* upstream enhancers is dependent on SOX9 in differentiated chondrocytes (Yao *et al.*, 2015). Prior to the onset of chondrogenesis SOX9 overexpression in MSCs didn't significantly induce *ROCR* expression (Supp. Fig. 7B), but we can't rule out that SOX9 may promote the expression of *ROCR* during chondrogenesis, or in adult chondrocytes. Despite knockdown of *ROCR* reducing SOX9 expression and cartilage gene expression in MSCs reciprocal overexpression of *ROCR* had no effect. Overexpression from an artificial plasmid transcription start site is not entirely analogous to endogenous *ROCR* expression with potential alteration to secondary structure formation and cellular localisation of the RNA.

During skeletogenesis MSC condensation initiates the formation of multipotent osteochondroprogenitors whose lineage fate is then determined by the combination of growth factor signals received. *ROCR* is only upregulated during chondrogenesis, not osteoblastogenesis, suggesting a key role in directing MSCs toward the chondrocyte lineage. Consistent with this only a minor impact of *ROCR* depletion was observed during MSC osteoblastogenesis in contrast to its key requirement during chondrogenesis. During osteochondroprogenitor differentiation SOX9 has antagonistic effects on the osteoblast transcription factor RUNX2 in determining the specific differentiation into their respective chondrocyte and osteoblast lineages (Zhou *et al.*, 2006). Owing to the lack of induction of *ROCR* during osteoblastogenesis, no effect would be expected. Interestingly, depletion of *SOX9-AS1* significantly reduced the expression of adipogenic marker genes, confirming the efficacy of the *SOX9-AS1* depletion and given the role of SOX9 in adipogenic differentiation suggests *SOX9-AS1* also contributes to the differentiation (Stockl *et al.*, 2013).

We demonstrated that returning SOX9 levels to normal by overexpression could reverse the impaired chondrogenesis phenotype caused by depletion of *ROCR*. This indicated that SOX9 can largely replace *ROCR* during MSC chondrogenesis as *SOX9* expression was sufficient to produce the cartilage matrix.

Thus, suggesting *ROCR* is indirectly needed in chondrogenesis to establish the correct level of *SOX9* expression in MSCs during differentiation. Both silencing and activating roles have been demonstrated for lncRNAs. *XIST* establishes X chromosome inactivation, while *RMST* facilitates SOX2 binding to promoter regions of neurogenic transcription factors (Vance and Ponting, 2014). In some cases enhancer regions and the process of transcription at the lncRNA locus facilitate downstream gene expression rather than the lncRNA transcript itself (Engreitz *et al.*, 2016). Our knockdown experiments indicate that *ROCR* transcript is functional, and the *ROCR* locus is considerably upstream from SOX9 (94kb), but we can't rule out that the ROCR locus may also function as an enhancer. Many of the identified functional lncRNA actions occur in the nucleus, however, *ROCR* appears to reside more in the cytoplasm than nucleus, indicating an indirect regulation of SOX9. Our coding analysis indicated *ROCR* is unlikely to code for any significant peptide transcript suggesting a role for the RNA in the cytoplasm. A number of cytoplasmic lncRNAs can regulate mRNA half-life and translation. *TINCR* is induced during epidermal differentiation and required for stability of differentiation mediators (Kretz *et al.*, 2013) and antisense *Uchl1* lncRNA promotes translation of *Uchl1* (Carrieri *et al.*, 2012). Other factors also contribute to cartilage gene expression, such as SP1 and forkhead/winged-helix domain (FOX) proteins, and may account for why despite normal GAG levels, the expression of *COL2A1* and *ACAN* was not completely restored during rescue by SOX9, again suggesting an indirect effect of *ROCR* (Liu *et al.*, 2016). Or this may simply reflect the difference in sampling time for gene expression in comparison to matrix GAG measurement. Almost all lncRNAs function through association with protein partners and accordingly RNA pulldown methods are commonly used to identify such interactions (Yang *et al.*, 2015).

Conservation of lncRNAs across species is low, with less than 10% of all lncRNAs exhibiting regions of conservation compared to random control regions (Iyer *et al.*, 2015), but there are key examples of conserved lncRNAs with critical roles in mouse development having human counterparts (Sauvageau *et al.*, 2013). By homology search for a mouse orthologue of *ROCR* we identified a predicted noncoding RNA transcript (NR_024085/BC006965) with sequence similarity to exon 2 of *ROCR* transcript variant 1 (exon 3 of variants 2 and 3), but little mammalian sequence conservation in general (Supp. Fig. 8). Importantly, the transcripts are in syntenic regions (containing *SOX9*) of human chromosome 17q24 and mouse 11qE2. By real-time RT-PCR of mouse cartilage RNA we have now confirmed the expression of a murine multiple exon version of *ROCR* (Supp. Fig. 8). Further work will establish whether the murine transcript is regulated during chondrogenesis and contributes to chondrocyte development.

Conclusions

The cartilage transcriptome contains many lncRNA transcripts many of which may have important functions in cartilage biology. Our identification of cartilage lncRNAs complements the previous identification of inflammation-induced lncRNAs in chondrocytes (Pearson *et al.*, 2016). This panel of chondocyte lncRNAs is specific to human aged hip cartilage and further work should establish the expression of lncRNAs specific to different zones of articular cartilage, as well as growth plate cartilage and to establish the impact of weight bearing, age and disease such as OA. Functional analysis indicated that *ROCR* was induced during chondrogenic differentiation and played an important role in the induction of *SOX9* and as a result cartilage gene expression. Because SOX9-expressing cells are progenitors for numerous tissues identifying chondrocyte-specific regulatory elements might aid understanding of differentiation of chondrocytes from MSCs, potentially useful in chondrocyte tissue engineering applications.

Methods

Human tissue isolation

Normal human articular cartilage was obtained from patients undergoing joint replacement surgery due to intracapsular neck of femur fracture (NOF). OA human articular cartilage was obtained from knee joint replacement operations on patients diagnosed with osteoarthritis (OA). Synovium and infrapatellar fat pad were also collected from the knee of OA patients. All tissue was obtained with informed consent and ethics committee approval from the Newcastle and North Tyneside Health Authority. Scoring, extraction and patient information for the NOF samples are detailed in Xu *et al.* (Xu *et al.*, 2012). Briefly, joints were inspected macroscopically and scored by blinded experience orthopaedic surgeon to identify normal NOF cartilage. Cartilage, all zones, was collected within 2 hours of surgery stored at −80°C prior to RNA extraction.

Human bone marrow MSC culture

Human bone marrow MSCs (from seven donors, 18-25 years of age) were isolated from human bone marrow mononuclear cells (Lonza Biosciences, Berkshire, UK) and cultured and phenotype-tested as described previously (Barter *et al.*, 2015). Experiments were performed using cells between P2-P7, and all experiments were repeated with cells from 3-4 donors.

Chondrogenic differentiation

MSC were resuspended in chondrogenic culture medium consisting of high glucose DMEM containing 100 µg/ml sodium pyruvate, 10 ng/ml TGF-β3, 100 nM dexamethasone, 1x ITS-1 premix, 40 µg/ml proline, and 25 µg/ml ascorbate-2-phosphate. $5x10^5$ MSC in 100µl medium were pipetted onto 6.5mm diameter, 0.4-µm pore size polycarbonate Transwell filters (Merck Millipore, Watford, UK), centrifuged at 200g for 5 minutes, then 0.5 ml of chondrogenic medium added to the lower well as described described previously (Murdoch *et al.*, 2007; Barter *et al.*, 2015). For V-bottom 96-well plate pellet chondrogenesis $5x10^4$ MSCs in 150µl chondrogenic medium were pipetted into a UV-sterilised V-bottom 96-well plate and centrifuged at 500 *g* for 5 minutes. Media were replaced every 2 or 3 days for up to 7 days.

Osteoblast and adipocyte differentiation

MSC were plated in 96-well plates at a density of 15000/cm^2 for 24 hours then media were replaced with either osteoblastogenic culture medium consisting of DMEM supplemented with 10% FBS v/v (foetal bovine serum), β-Glycerol Phosphate (10mM), dexamethasone (100nM) and ascorbic acid 2-phosphate (50ug/ml), or adipogenic culture medium consisting of DMEM supplemented with 10% FBS, dexamethasone (1µM), insulin (10µg/ml), IBMX (0.5mM), indomethacin (60µM), rosiglitazone (2µM) and IGF-1 (20nM; R&D Systems) (all Sigma unless specified). Media were replaced every 3 or 4 days. 7 days of differentiation was sufficient to assess gene expression changes in markers of differentiation. Cells were cultured for 21 days in osteoblastogenic medium to achieve fully mineralized cultures, and for 14 days in adipogenic medium for lipid production.

Histology and biochemical analysis

Transwell discs were stained as described (Barter *et al.*, 2015). Chondrogenic pellets and transwell discs were digested with papain (10U/ml) at 60°C (Murdoch *et al.*, 2007). The sulphated glycosaminoglycan (GAG) content was measured by 1,9-dimethylmethylene blue binding (Sigma) using chondroitin sulphate (Sigma) as standard (Farndale *et al.*, 1982), and the DNA content was measured with PicoGreen (Invitrogen) intercalating dye following the manufacturer's instructions. Cells undergoing osteoblast differentiation were fixed in 70% cold EtOH (5 minutes, -20°C). After drying the wells to reveal calcium-rich mineralisation deposits the cells were incubated at room temperature with a solution of Alizarin Red (Sigma) (40 mM, pH 4.2) for 20-30 minutes. For quantification the staining was extracted with 10% (w/v) Cetylpyridinium (Sigma) solubilized in 10 mM sodium phosphate buffer (pH 7) and the absorbance measured at 620nM. Cells undergoing adipogenesis were fixed with formalin for 1 hour, washed with distilled water and 60% isopropanol

then dried. To reveal the presence of lipid droplets the cells were stained with a 21% (w/v) solution of Oil Red O for 10 minutes. For quantitation the staining was extracted with 100% isopropanol and the absorbance measured at 500nM. Stained cells were washed with distilled water prior to image acquisition.

RNA extraction and real-time reverse transcription PCR

Cartilage, synovium and fat pad samples were ground into powder and homogenized using Invitrogen TRIzol Reagent (Life Technologies, Paisley, UK) prior to RNA purification using the Qiagen RNeasy mini kit (Qiagen, Crawley, UK) essentially as previously described (Xu *et al.*, 2012). MSC chondrogenic transwell discs were disrupted in TRIzol (for real-time RT-PCR) using a small disposable plastic pestle and an aliquot of Molecular Grinding Resin (G-Biosciences/Genotech, St. Louis). MSC chondrogenesis pellets were disrupted in Ambion Cells-to-cDNA II Cell Lysis buffer (Life Technologies). Total RNA was then extracted and converted to cDNA using MMLV reverse transcriptase (Invitrogen) and TaqMan real-time RT-PCR was performed and gene expression levels were calculated as described previously (Barter *et al.*, 2010). Nuclear and cytoplasmic RNA fractions were separated using the CelLytic NuCLEAR Extraction Kit (Sigma) supplemented with RNaseOUT ribonuclease inhibitor (Life Technologies). All values are presented as the mean ± SEM of replicates in pooled experiments. lncRNA real-time RT-PCR amplification products were sequence verified by cloning into the pCR4-TOPO vector (Life Technologies). Ambion FirstChoice Human Total RNA Survey Panel (AM6000) contains pools of total RNA from 20 different normal human tissues, each pool consisting of RNA from at least 3 tissue donors. Primer sequences are located in Table 1.

RNA-Seq and analysis

RNA integrity was checked using an Agilent Bioanalyzer 2100 (Agilent Technologies, Santa Clara, California); RNA samples with an RNA Integrity Number (RIN) ≥ 7 were selected. For each sample cDNA libraries were prepared for sequencing from 5µg of total RNA using Illumina TrueSeq mRNA kits with the manufacturers' protocols. mRNA enriched RNA was initially purified using polydT oligo attached magnetic beads using two rounds of purification. During the second elution the RNA was fragmented and random primed for cDNA synthesis. After the addition of a single 'A' base adaptors were annealed, and the products purified and enriched with PCR to create a final cDNA library. No indexing (barcoding) was performed. Library DNA size was checked using the Agilent Bioanalyzer and quantified using the Kapa Library Quant kits (Kapa Biosciences). A 7.5pM solution of each library was loaded onto each lane of an Illumina Genome Analyzer IIa and 78-base paired-end sequencing performed. On average each sample gave 28 million read pairs. Sample quality control was performed using FastQC (Babraham Bioinformatics). Reads were aligned to the reference genome using TopHat, specifying mate inner distance (mean inner distance between mate pairs) and standard deviation for each

sample (Trapnell *et al.*, 2012). Mapped reads were then assembled into complete transcripts using the splice junction mapping tool Cufflinks, with option –G which utilises the Ensembl reference gene track to improve mapping. Cuffmerge was used to merge the assembled transcripts into a consensus gene track from the all of the mapped samples. Ensembl transcript biotypes were applied to identify lncRNAs (biotype lincRNA). Coding potential of lncRNAs was assessed with ORFfinder (NCBI), Coding Potential Assessment Tool (CPAT), Coding Potential Calculator (CPC) and PhyloCSF (Kong *et al.*, 2007; Lin *et al.*, 2011; Wang *et al.*, 2013). RNA sequencing has been uploaded to GEO.

RNA-mediated interference, GapmeR transfection and lentiviral transduction

For siRNA transfection 50nM siRNA was transfected into 40-50% confluent MSCs using Dharmafect™ 1 lipid reagent (Thermo Fisher). 50nM siRNA Dharmacon siGENOME and ON-TARGET+ siRNA (Thermo Fisher Scientific, Lafayette, CO.) were used to target *SOX9-AS1* and *ROCR*. Depletion of gene-specific mRNA levels was calculated by comparison of expression levels with cells transfected with 50nM siCONTROL (non-targeting siRNA 2, cat. 001210-02; Dharmacon). For GapmeR transfection 100nM Antisense LNA GapmeR (Exiqon, Vedbaek, Denmark) targetting *ROCR* or non-targetting control (Negative Control A, cat. 300610) were transfected as for siRNAs. siRNA and GapmeR sequences are located in Table 1. pCDH-EF1-MCS-IRES-copGFP lentivirus expression vector (System Biosciences, Palo Alto, CA) containing SOX9 was generated by cloning SOX9 from pUT-FLAG-SOX9 (Lefebvre *et al.*, 1997). pCDH-EF1-MCS lentivirus expression vectors containing ROCR transcript variant 2 and transcript variant 3 were generated by cloning gBlock gene fragments (IDT) containing the sequences specified in Supp. Fig 1. Lentiviruses expressing SOX9, ROCR or control empty vector lentivirus were generated by transfecting HEK-293T cells with pCDH plasmids, together with packaging plasmids pCMV-VSV-G and psPAX2 (Addgene #8454 and #12260). The virus-containing culture media were collected every 24 hours for 3 days and concentrated (10x) with Clontech Lenti-X Concentrator into PBS (Takara, Mountain View, CA). MSCs and HAC were transduced with the lentivirus-containing PBS plus 8 µg/ml polybrene. A Promega CytoTox 96 cytotoxicity assay was used to assess cell viability following siRNA treatment (Supp. Fig. 8).

Rapid amplification of cDNA ends (RACE)

5'RACE was performed on RNA extracted from human articular cartilage or MSCs using the Invitrogen 5' RACE System for Rapid Amplification of cDNA Ends (Life Technologies). Primer sequences are listed in Supp. Table 1. PCR amplification products were electrophoresed on agarose gels, cloned into the pCR4-TOPO vector and Sanger sequenced. The sequences have been uploaded to GenBank.

Immunoblotting

Lysates from MSCs were prepared as described previously (Barter *et al.*, 2010). Lysates were immunoblotted with the following antibodies: SOX9 (AB5535, 1:2000 dilution) and GAPDH (AB2302, 1:40000 dilution) (both Merck Millipore). Secondary anti-rabbit antibodies were from Dako (Ely, UK) and chemiluminescent images were captured using a G:BOX Chemi system (Syngene, Cambridge, UK).

Statistical analysis

Data from each donor was individually analysed for gene expression and the values from each donor were then pooled to generate the mean± SEM. Significant differences between sample groups were assessed by one-way analysis of variance followed by the Bonferroni post hoc test for multiple comparisons or a two-tailed Students *t*-test was performed for single comparisons.

References

Akiyama, H. (2008) 'Control of chondrogenesis by the transcription factor Sox9', *Mod Rheumatol*, 18(3), pp. 213-9.

Akiyama, H., Chaboissier, M.C., Martin, J.F., Schedl, A. and de Crombrugghe, B. (2002) 'The transcription factor Sox9 has essential roles in successive steps of the chondrocyte differentiation pathway and is required for expression of Sox5 and Sox6', *Genes Dev*, 16(21), pp. 2813-28.

Akiyama, H. and Lefebvre, V. (2011) 'Unraveling the transcriptional regulatory machinery in chondrogenesis', *J Bone Miner Metab*, 29(4), pp. 390-5.

Barter, M.J., Hui, W., Lakey, R.L., Catterall, J.B., Cawston, T.E. and Young, D.A. (2010) 'Lipophilic statins prevent matrix metalloproteinase-mediated cartilage collagen breakdown by inhibiting protein geranylgeranylation', *Ann Rheum Dis*, 69(12), pp. 2189-98.

Barter, M.J., Tselepi, M., Gomez, R., Woods, S., Hui, W., Smith, G.R., Shanley, D.P., Clark, I.M. and Young, D.A. (2015) 'Genome-Wide MicroRNA and Gene Analysis of Mesenchymal Stem Cell Chondrogenesis Identifies an Essential Role and Multiple Targets for miR-140-5p', *Stem Cells*, 33(11), pp. 3266-80.

Carlson, H.L., Quinn, J.J., Yang, Y.W., Thornburg, C.K., Chang, H.Y. and Stadler, H.S. (2015) 'LncRNA-HIT Functions as an Epigenetic Regulator of Chondrogenesis through Its Recruitment of p100/CBP Complexes', *PLoS Genet*, 11(12), p. e1005680.

Carrieri, C., Cimatti, L., Biagioli, M., Beugnet, A., Zucchelli, S., Fedele, S., Pesce, E., Ferrer, I., Collavin, L., Santoro, C., Forrest, A.R., Carninci, P., Biffo, S., Stupka, E. and Gustincich, S. (2012) 'Long non-coding antisense RNA controls Uchl1 translation through an embedded SINEB2 repeat', *Nature*, 491(7424), pp. 454-7.

Chimal-Monroy, J., Rodriguez-Leon, J., Montero, J.A., Ganan, Y., Macias, D., Merino, R. and Hurle, J.M. (2003) 'Analysis of the molecular cascade responsible for mesodermal limb chondrogenesis: Sox genes and BMP signaling', *Dev Biol*, 257(2), pp. 292-301.

Consortium, E.P. (2012) 'An integrated encyclopedia of DNA elements in the human genome', *Nature*, 489(7414), pp. 57-74.

Derrien, T., Johnson, R., Bussotti, G., Tanzer, A., Djebali, S., Tilgner, H., Guernec, G., Martin, D., Merkel, A., Knowles, D.G., Lagarde, J., Veeravalli, L., Ruan, X., Ruan, Y., Lassmann, T., Carninci, P., Brown, J.B., Lipovich, L., Gonzalez, J.M., Thomas, M., Davis, C.A., Shiekhattar, R., Gingeras, T.R., Hubbard, T.J., Notredame, C., Harrow, J. and Guigo, R. (2012) 'The GENCODE v7 catalog of human long noncoding RNAs: analysis of their gene structure, evolution, and expression', *Genome Res*, 22(9), pp. 1775-89.

Dunn, S.L., Soul, J., Anand, S., Schwartz, J.M., Boot-Handford, R.P. and Hardingham, T.E. (2016) 'Gene expression changes in damaged osteoarthritic cartilage identify a signature of non-chondrogenic and mechanical responses', *Osteoarthritis Cartilage*, 24(8), pp. 1431-40.

Engreitz, J.M., Haines, J.E., Perez, E.M., Munson, G., Chen, J., Kane, M., McDonel, P.E., Guttman, M. and Lander, E.S. (2016) 'Local regulation of gene expression by lncRNA promoters, transcription and splicing', *Nature*, 539(7629), pp. 452-455.

Ernst, J., Kheradpour, P., Mikkelsen, T.S., Shoresh, N., Ward, L.D., Epstein, C.B., Zhang, X., Wang, L., Issner, R., Coyne, M., Ku, M., Durham, T., Kellis, M. and Bernstein, B.E. (2011) 'Mapping and analysis of chromatin state dynamics in nine human cell types', *Nature*, 473(7345), pp. 43-9.

Fagerberg, L., Hallstrom, B.M., Oksvold, P., Kampf, C., Djureinovic, D., Odeberg, J., Habuka, M., Tahmasebpoor, S., Danielsson, A., Edlund, K., Asplund, A., Sjostedt, E., Lundberg, E., Szigyarto, C.A., Skogs, M., Takanen, J.O., Berling, H., Tegel, H., Mulder, J., Nilsson, P., Schwenk, J.M., Lindskog, C., Danielsson, F., Mardinoglu, A., Sivertsson, A., von Feilitzen, K., Forsberg, M., Zwahlen, M., Olsson, I., Navani, S., Huss, M., Nielsen, J., Ponten, F. and Uhlen, M. (2014) 'Analysis of the human tissue-

specific expression by genome-wide integration of transcriptomics and antibody-based proteomics', *Mol Cell Proteomics*, 13(2), pp. 397-406.
Farndale, R.W., Sayers, C.A. and Barrett, A.J. (1982) 'A direct spectrophotometric microassay for sulfated glycosaminoglycans in cartilage cultures', *Connect Tissue Res*, 9(4), pp. 247-8.
Fatica, A. and Bozzoni, I. (2014) 'Long non-coding RNAs: new players in cell differentiation and development', *Nat Rev Genet*, 15(1), pp. 7-21.
Flicek, P., Amode, M.R., Barrell, D., Beal, K., Billis, K., Brent, S., Carvalho-Silva, D., Clapham, P., Coates, G., Fitzgerald, S., Gil, L., Giron, C.G., Gordon, L., Hourlier, T., Hunt, S., Johnson, N., Juettemann, T., Kahari, A.K., Keenan, S., Kulesha, E., Martin, F.J., Maurel, T., McLaren, W.M., Murphy, D.N., Nag, R., Overduin, B., Pignatelli, M., Pritchard, B., Pritchard, E., Riat, H.S., Ruffier, M., Sheppard, D., Taylor, K., Thormann, A., Trevanion, S.J., Vullo, A., Wilder, S.P., Wilson, M., Zadissa, A., Aken, B.L., Birney, E., Cunningham, F., Harrow, J., Herrero, J., Hubbard, T.J., Kinsella, R., Muffato, M., Parker, A., Spudich, G., Yates, A., Zerbino, D.R. and Searle, S.M. (2014) 'Ensembl 2014', *Nucleic Acids Res*, 42(Database issue), pp. D749-55.
Foster, J.W., Dominguez-Steglich, M.A., Guioli, S., Kwok, C., Weller, P.A., Stevanovic, M., Weissenbach, J., Mansour, S., Young, I.D., Goodfellow, P.N. and et al. (1994) 'Campomelic dysplasia and autosomal sex reversal caused by mutations in an SRY-related gene', *Nature*, 372(6506), pp. 525-30.
Gordon, C.T., Tan, T.Y., Benko, S., Fitzpatrick, D., Lyonnet, S. and Farlie, P.G. (2009) 'Long-range regulation at the SOX9 locus in development and disease', *J Med Genet*, 46(10), pp. 649-56.
Huynh, N.P., Anderson, B.A., Guilak, F. and McAlinden, A. (2017) 'Emerging roles for long noncoding RNAs in skeletal biology and disease', *Connect Tissue Res*, 58(1), pp. 116-141.
Iyer, M.K., Niknafs, Y.S., Malik, R., Singhal, U., Sahu, A., Hosono, Y., Barrette, T.R., Prensner, J.R., Evans, J.R., Zhao, S., Poliakov, A., Cao, X., Dhanasekaran, S.M., Wu, Y.M., Robinson, D.R., Beer, D.G., Feng, F.Y., Iyer, H.K. and Chinnaiyan, A.M. (2015) 'The landscape of long noncoding RNAs in the human transcriptome', *Nat Genet*, 47(3), pp. 199-208.
Kawakami, Y., Rodriguez-Leon, J. and Izpisua Belmonte, J.C. (2006) 'The role of TGFbetas and Sox9 during limb chondrogenesis', *Curr Opin Cell Biol*, 18(6), pp. 723-9.
Klattenhoff, C.A., Scheuermann, J.C., Surface, L.E., Bradley, R.K., Fields, P.A., Steinhauser, M.L., Ding, H., Butty, V.L., Torrey, L., Haas, S., Abo, R., Tabebordbar, M., Lee, R.T., Burge, C.B. and Boyer, L.A. (2013) 'Braveheart, a long noncoding RNA required for cardiovascular lineage commitment', *Cell*, 152(3), pp. 570-83.
Kong, L., Zhang, Y., Ye, Z.Q., Liu, X.Q., Zhao, S.Q., Wei, L. and Gao, G. (2007) 'CPC: assess the protein-coding potential of transcripts using sequence features and support vector machine', *Nucleic Acids Res*, 35(Web Server issue), pp. W345-9.
Kretz, M., Siprashvili, Z., Chu, C., Webster, D.E., Zehnder, A., Qu, K., Lee, C.S., Flockhart, R.J., Groff, A.F., Chow, J., Johnston, D., Kim, G.E., Spitale, R.C., Flynn, R.A., Zheng, G.X., Aiyer, S., Raj, A., Rinn, J.L., Chang, H.Y. and Khavari, P.A. (2013) 'Control of somatic tissue differentiation by the long non-coding RNA TINCR', *Nature*, 493(7431), pp. 231-5.
Krupp, M., Marquardt, J.U., Sahin, U., Galle, P.R., Castle, J. and Teufel, A. (2012) 'RNA-Seq Atlas--a reference database for gene expression profiling in normal tissue by next-generation sequencing', *Bioinformatics*, 28(8), pp. 1184-5.
Lefebvre, V. and Dvir-Ginzberg, M. (2017) 'SOX9 and the many facets of its regulation in the chondrocyte lineage', *Connect Tissue Res*, 58(1), pp. 2-14.
Lefebvre, V., Huang, W., Harley, V.R., Goodfellow, P.N. and de Crombrugghe, B. (1997) 'SOX9 is a potent activator of the chondrocyte-specific enhancer of the pro alpha1(II) collagen gene', *Mol Cell Biol*, 17(4), pp. 2336-46.
Leipoldt, M., Erdel, M., Bien-Willner, G.A., Smyk, M., Theurl, M., Yatsenko, S.A., Lupski, J.R., Lane, A.H., Shanske, A.L., Stankiewicz, P. and Scherer, G. (2007) 'Two novel translocation breakpoints upstream of SOX9 define borders of the proximal and distal breakpoint cluster region in campomelic dysplasia', *Clin Genet*, 71(1), pp. 67-75.

Li, L., Liu, B., Wapinski, O.L., Tsai, M.C., Qu, K., Zhang, J., Carlson, J.C., Lin, M., Fang, F., Gupta, R.A., Helms, J.A. and Chang, H.Y. (2013) 'Targeted disruption of Hotair leads to homeotic transformation and gene derepression', *Cell Rep*, 5(1), pp. 3-12.
Lin, M.F., Jungreis, I. and Kellis, M. (2011) 'PhyloCSF: a comparative genomics method to distinguish protein coding and non-coding regions', *Bioinformatics*, 27(13), pp. i275-82.
Liu, C.F., Samsa, W.E., Zhou, G. and Lefebvre, V. (2016) 'Transcriptional control of chondrocyte specification and differentiation', *Semin Cell Dev Biol*.
Maass, P.G., Rump, A., Schulz, H., Stricker, S., Schulze, L., Platzer, K., Aydin, A., Tinschert, S., Goldring, M.B., Luft, F.C. and Bahring, S. (2012) 'A misplaced lncRNA causes brachydactyly in humans', *J Clin Invest*, 122(11), pp. 3990-4002.
Mansour, S., Offiah, A.C., McDowall, S., Sim, P., Tolmie, J. and Hall, C. (2002) 'The phenotype of survivors of campomelic dysplasia', *J Med Genet*, 39(8), pp. 597-602.
Mead, T.J., Wang, Q., Bhattaram, P., Dy, P., Afelik, S., Jensen, J. and Lefebvre, V. (2013) 'A far-upstream (-70 kb) enhancer mediates Sox9 auto-regulation in somatic tissues during development and adult regeneration', *Nucleic Acids Res*, 41(8), pp. 4459-69.
Murdoch, A.D., Grady, L.M., Ablett, M.P., Katopodi, T., Meadows, R.S. and Hardingham, T.E. (2007) 'Chondrogenic differentiation of human bone marrow stem cells in transwell cultures: generation of scaffold-free cartilage', *Stem Cells*, 25(11), pp. 2786-96.
Ng, S.Y., Bogu, G.K., Soh, B.S. and Stanton, L.W. (2013) 'The long noncoding RNA RMST interacts with SOX2 to regulate neurogenesis', *Mol Cell*, 51(3), pp. 349-59.
Ninomiya, S., Isomura, M., Narahara, K., Seino, Y. and Nakamura, Y. (1996) 'Isolation of a testis-specific cDNA on chromosome 17q from a region adjacent to the breakpoint of t(12;17) observed in a patient with acampomelic campomelic dysplasia and sex reversal', *Hum Mol Genet*, 5(1), pp. 69-72.
Onyekwelu, I., Goldring, M.B. and Hidaka, C. (2009) 'Chondrogenesis, joint formation, and articular cartilage regeneration', *J Cell Biochem*, 107(3), pp. 383-92.
Orom, U.A., Derrien, T., Beringer, M., Gumireddy, K., Gardini, A., Bussotti, G., Lai, F., Zytnicki, M., Notredame, C., Huang, Q., Guigo, R. and Shiekhattar, R. (2010) 'Long noncoding RNAs with enhancer-like function in human cells', *Cell*, 143(1), pp. 46-58.
Pearson, M.J., Philp, A.M., Heward, J.A., Roux, B.T., Walsh, D.A., Davis, E.T., Lindsay, M.A. and Jones, S.W. (2016) 'Long Intergenic Noncoding RNAs Mediate the Human Chondrocyte Inflammatory Response and Are Differentially Expressed in Osteoarthritis Cartilage', *Arthritis Rheumatol*, 68(4), pp. 845-56.
Perry, R.B. and Ulitsky, I. (2016) 'The functions of long noncoding RNAs in development and stem cells', *Development*, 143(21), pp. 3882-3894.
Pittenger, M.F., Mackay, A.M., Beck, S.C., Jaiswal, R.K., Douglas, R., Mosca, J.D., Moorman, M.A., Simonetti, D.W., Craig, S. and Marshak, D.R. (1999) 'Multilineage potential of adult human mesenchymal stem cells', *Science*, 284(5411), pp. 143-7.
Pritchett, J., Athwal, V., Roberts, N., Hanley, N.A. and Hanley, K.P. (2011) 'Understanding the role of SOX9 in acquired diseases: lessons from development', *Trends Mol Med*, 17(3), pp. 166-74.
Quinodoz, S. and Guttman, M. (2014) 'Long noncoding RNAs: an emerging link between gene regulation and nuclear organization', *Trends Cell Biol*, 24(11), pp. 651-663.
Rinn, J.L. and Chang, H.Y. (2012) 'Genome regulation by long noncoding RNAs', *Annu Rev Biochem*, 81, pp. 145-66.
Sauvageau, M., Goff, L.A., Lodato, S., Bonev, B., Groff, A.F., Gerhardinger, C., Sanchez-Gomez, D.B., Hacisuleyman, E., Li, E., Spence, M., Liapis, S.C., Mallard, W., Morse, M., Swerdel, M.R., D'Ecclessis, M.F., Moore, J.C., Lai, V., Gong, G., Yancopoulos, G.D., Frendewey, D., Kellis, M., Hart, R.P., Valenzuela, D.M., Arlotta, P. and Rinn, J.L. (2013) 'Multiple knockout mouse models reveal lincRNAs are required for life and brain development', *Elife*, 2, p. e01749.
Sekiya, I., Vuoristo, J.T., Larson, B.L. and Prockop, D.J. (2002) 'In vitro cartilage formation by human adult stem cells from bone marrow stroma defines the sequence of cellular and molecular events during chondrogenesis', *Proc Natl Acad Sci U S A*, 99(7), pp. 4397-402.

Stockl, S., Bauer, R.J., Bosserhoff, A.K., Gottl, C., Grifka, J. and Grassel, S. (2013) 'Sox9 modulates cell survival and adipogenic differentiation of multipotent adult rat mesenchymal stem cells', *J Cell Sci*, 126(Pt 13), pp. 2890-902.
Trapnell, C., Roberts, A., Goff, L., Pertea, G., Kim, D., Kelley, D.R., Pimentel, H., Salzberg, S.L., Rinn, J.L. and Pachter, L. (2012) 'Differential gene and transcript expression analysis of RNA-seq experiments with TopHat and Cufflinks', *Nat Protoc*, 7(3), pp. 562-78.
Ulitsky, I., Shkumatava, A., Jan, C.H., Sive, H. and Bartel, D.P. (2011) 'Conserved function of lincRNAs in vertebrate embryonic development despite rapid sequence evolution', *Cell*, 147(7), pp. 1537-50.
Vance, K.W. and Ponting, C.P. (2014) 'Transcriptional regulatory functions of nuclear long noncoding RNAs', *Trends Genet*, 30(8), pp. 348-55.
Wagner, T., Wirth, J., Meyer, J., Zabel, B., Held, M., Zimmer, J., Pasantes, J., Bricarelli, F.D., Keutel, J., Hustert, E., Wolf, U., Tommerup, N., Schempp, W. and Scherer, G. (1994) 'Autosomal sex reversal and campomelic dysplasia are caused by mutations in and around the SRY-related gene SOX9', *Cell*, 79(6), pp. 1111-20.
Wang, K.C., Yang, Y.W., Liu, B., Sanyal, A., Corces-Zimmerman, R., Chen, Y., Lajoie, B.R., Protacio, A., Flynn, R.A., Gupta, R.A., Wysocka, J., Lei, M., Dekker, J., Helms, J.A. and Chang, H.Y. (2011) 'A long noncoding RNA maintains active chromatin to coordinate homeotic gene expression', *Nature*, 472(7341), pp. 120-4.
Wang, L., Park, H.J., Dasari, S., Wang, S., Kocher, J.P. and Li, W. (2013) 'CPAT: Coding-Potential Assessment Tool using an alignment-free logistic regression model', *Nucleic Acids Res*, 41(6), p. e74.
Wright, E., Hargrave, M.R., Christiansen, J., Cooper, L., Kun, J., Evans, T., Gangadharan, U., Greenfield, A. and Koopman, P. (1995) 'The Sry-related gene Sox9 is expressed during chondrogenesis in mouse embryos', *Nat Genet*, 9(1), pp. 15-20.
Wunderle, V.M., Critcher, R., Hastie, N., Goodfellow, P.N. and Schedl, A. (1998) 'Deletion of long-range regulatory elements upstream of SOX9 causes campomelic dysplasia', *Proc Natl Acad Sci U S A*, 95(18), pp. 10649-54.
Xu, Y., Barter, M.J., Swan, D.C., Rankin, K.S., Rowan, A.D., Santibanez-Koref, M., Loughlin, J. and Young, D.A. (2012) 'Identification of the pathogenic pathways in osteoarthritic hip cartilage: commonality and discord between hip and knee OA', *Osteoarthritis Cartilage*, 20(9), pp. 1029-38.
Yang, Y., Wen, L. and Zhu, H. (2015) 'Unveiling the hidden function of long non-coding RNA by identifying its major partner-protein', *Cell Biosci*, 5, p. 59.
Yao, B., Wang, Q., Liu, C.F., Bhattaram, P., Li, W., Mead, T.J., Crish, J.F. and Lefebvre, V. (2015) 'The SOX9 upstream region prone to chromosomal aberrations causing campomelic dysplasia contains multiple cartilage enhancers', *Nucleic Acids Res*, 43(11), pp. 5394-408.
Yoon, B.S., Ovchinnikov, D.A., Yoshii, I., Mishina, Y., Behringer, R.R. and Lyons, K.M. (2005) 'Bmpr1a and Bmpr1b have overlapping functions and are essential for chondrogenesis in vivo', *Proc Natl Acad Sci U S A*, 102(14), pp. 5062-7.
Zhang, L., Chen, S., Bao, N., Yang, C., Ti, Y., Zhou, L. and Zhao, J. (2015) 'Sox4 enhances chondrogenic differentiation and proliferation of human synovium-derived stem cell via activation of long noncoding RNA DANCR', *J Mol Histol*, 46(6), pp. 467-73.
Zhou, G., Zheng, Q., Engin, F., Munivez, E., Chen, Y., Sebald, E., Krakow, D. and Lee, B. (2006) 'Dominance of SOX9 function over RUNX2 during skeletogenesis', *Proc Natl Acad Sci U S A*, 103(50), pp. 19004-9.

Figures

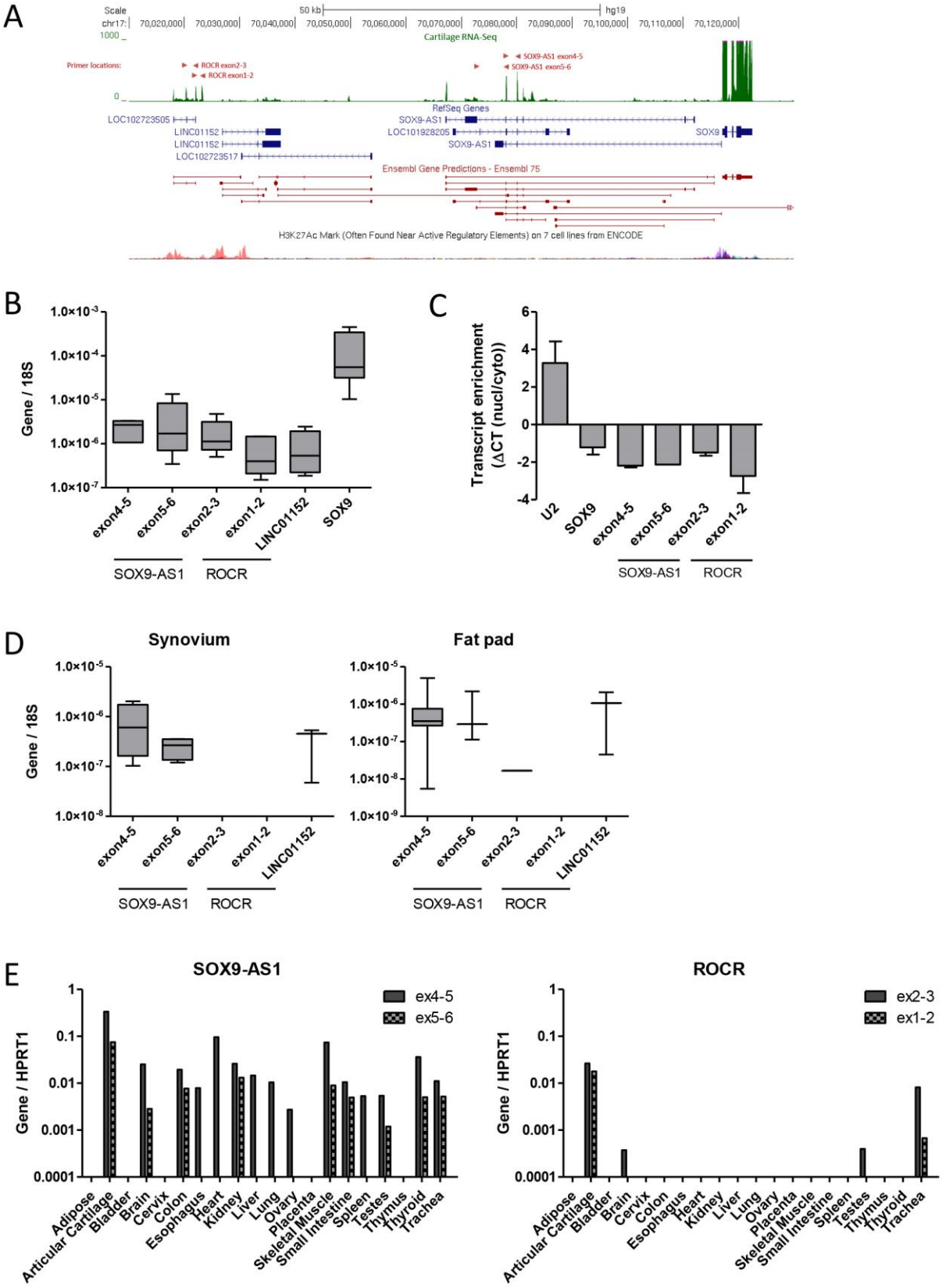

Figure 1. Expression of lncRNAs from the SOX9 locus

A. UCSC genome browser schematic of cartilage RNA-Seq reads aligned to the human genome with RefSeq gene annotations, Ensembl gene predictions and active H3K27Ac chromatin marks. Reads are pooled from 6 neck of femur (NOF) fracture cartilage donors. Primer locations are indicated by red arrowheads. B. Expression of *SOX9* locus lncRNAs and *SOX9* in RNA extracted from OA cartilage measured by real-time RT-PCR normalised to 18S. Values are the mean ± SEM of data pooled from 5 separate donors. C. Subcellular localisation of *SOX9-AS1* and *ROCR* in comparison with small nuclear RNA *U2* and *SOX9* mRNA pooled from 2 OA HAC donors. Values are the mean ± SEM of ΔCT between an equal fraction of nuclear and cytoplasmic RNA. D. Expression of *SOX9-AS1* and *ROCR* in RNA extracted from OA synovium and joint fat pad. Values are the mean ± SEM of data pooled from 8 separate synovium and fat pad donors. E. Expression of *SOX9-AS1* and *ROCR* in an RNA tissue panel measured. Values are the technical mean of data pooled from 3 donors per tissue.

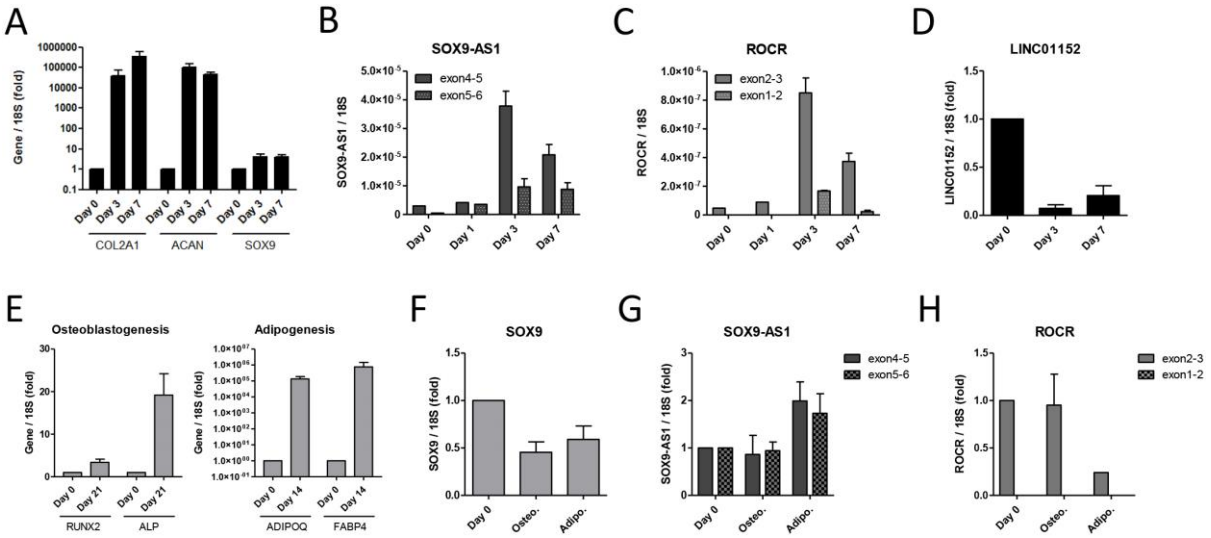

Figure 2. Expression of lncRNAs during MSC differentiation

A. Expression of the indicated genes in RNA extracted from MSCs undergoing chondrogenic differentiation at the indicated timepoints between Day 0 and Day 7. B-D. Expression of (B) *SOX9-AS1*, (C) *ROCR* and (D) *LINC01152* during MSC chondrogenic differentiation. E. Expression of the indicated genes in RNA extracted from MSCs undergoing osteoblastogenic and adipogenic differentiation. F-H. Expression of (F) *SOX9*, (G) *SOX9-AS1* and (H) *ROCR* during MSC osteoblastogenic and adipogenic differentiation. Values are the mean ± SEM of data pooled from 3-4 MSC donors.

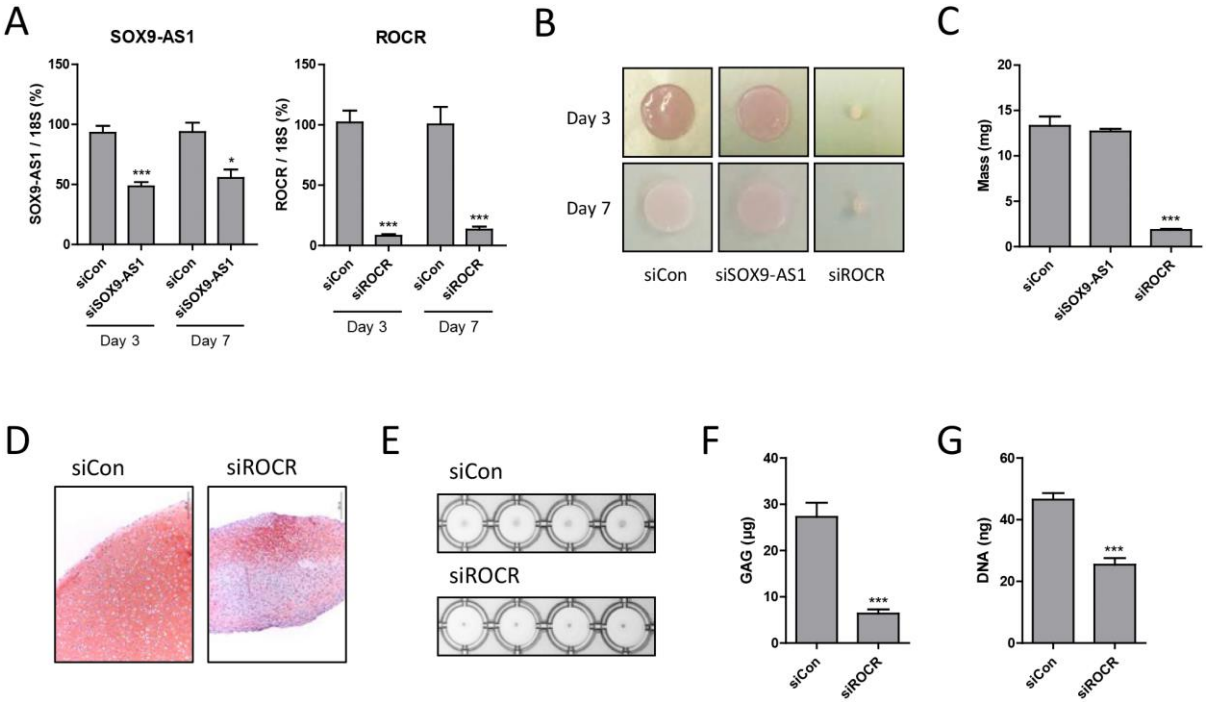

Figure 3. Effect of lncRNA depletion on MSC chondrogenic differentiation

A-D. MSCs were transfected for 2 days with *SOX9-AS1* or *ROCR*-targetting or non-targetting control siRNA prior to chondrogenic differentiation in hanging transwell inserts. A. *SOX9-AS1* and *ROCR* expression in RNA extracted from Day 3 and Day 7 chondrogenic discs. Expression is presented as a percentage of non-targetting control levels. B. Representative Day 3 and 7 chondrogenic discs. C. Wet mass of Day 7 chondrogenic discs. D. Representative Safranin O staining of Day 7 chondrogenic discs. E-F. MSCs were transfected for 1 day with *ROCR*-targetting or non-targetting control siRNA prior to chondrogenic differentiation in a V-bottom 96 well plate. E. Representative Day 7 chondrogenic pellets. F. GAG levels assayed by DMB assay in Day 7 chondrogenic pellets. G. DNA quantification by PicoGreen assay in Day 7 chondrogenic pellets. Values are the mean ± SEM of data pooled from (A-D) 3 MSC donors; (E-F) 4 MSC donors. ∗ = $P < 0.05$; ∗∗∗ = $P < 0.001$ for lncRNA siRNA versus non-targetting siRNA. Significant differences between sample groups were assessed by one-way analysis of variance followed by the Bonferroni post hoc test for multiple comparisons or a two-tailed Students *t*-test was performed for single comparisons.

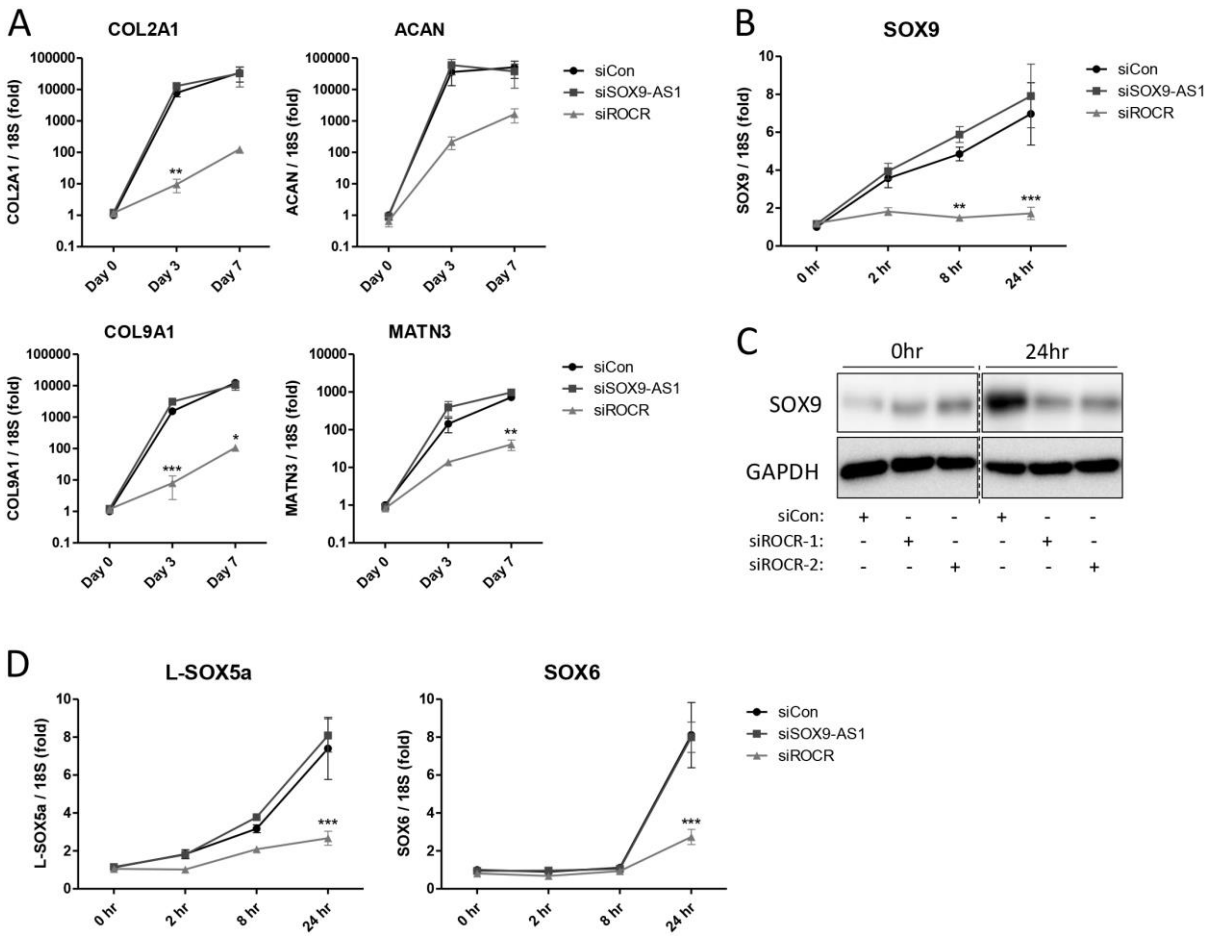

Figure 4. Effect of lncRNA depletion on MSC chondrogenic gene expression

A. MSCs were transfected for 2 days with *SOX9-AS1* or *ROCR*-targetting or non-targetting control siRNA prior to chondrogenic differentiation in hanging transwell inserts. RNA was extracted and expression of the indicated genes measured by real-time RT-PCR. B-D. MSCs were transfected for 1 day with *SOX9-AS1* or *ROCR*-targetting or non-targetting control siRNA prior to chondrogenic differentiation in a V-bottom 96 well plate for up to 24 hrs. RNA and protein was extracted and expression of *SOX9* (B) mRNA or (C) protein measured by real-time RT-PCR or immunoblotting. D. Expression of L-SOX5a and SOX6. Values are the mean ± SEM of data pooled from (A) 3 MSC donors; (B-D) 4 MSC donors. ∗ = P < 0.05; ∗∗ = P < 0.01; ∗∗∗ = P < 0.001 for lncRNA siRNA versus non-targetting siRNA. Significant differences between sample groups were assessed by one-way analysis of variance followed by the Bonferroni post hoc test for multiple comparisons or a two-tailed Students *t*-test was performed for single comparisons.

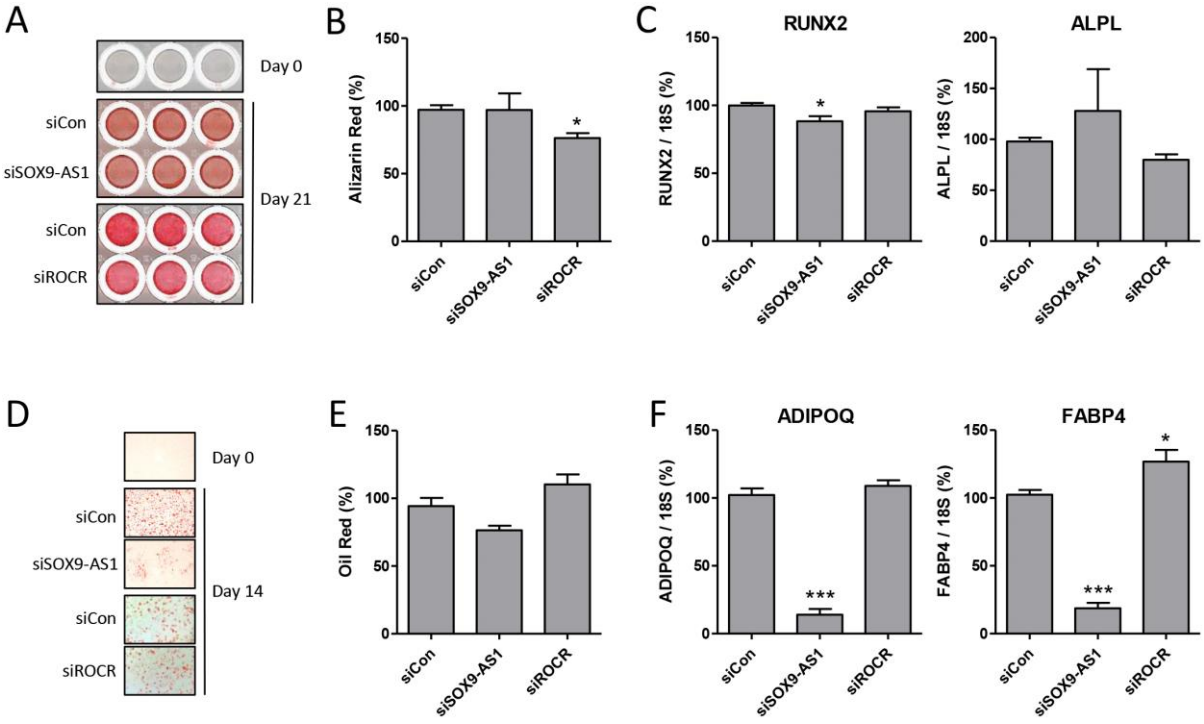

Figure 5. Effect of lncRNA depletion on MSC osteoblastogenic and adipogenic differentiation

A-C. MSCs were transfected for 2 days with *SOX9-AS1* or *ROCR*-targetting or non-targetting control siRNA prior to osteoblastogenic differentiation. A. Representative matrix mineralisation assayed by alizarin red staining after 21 days. B. Quantification of A. C. RNA was extracted and expression of the indicated genes at Day 7 measured by real-time RT-PCR. D-F. MSCs were transfected for 2 days with *SOX9-AS1* or *ROCR*-targetting or non-targetting control siRNA prior to adipogenic differentiation. D. Representative fat droplet generation assayed by oil red staining after 14 days. E. Quantification of D. F. RNA was extracted and expression of the indicated genes at Day 7 measured by real-time RT-PCR. Values are the mean ± SEM of data pooled from 4 MSC donors. ∗ = $P < 0.05$; ∗∗∗ = $P < 0.001$ for lncRNA siRNA versus non-targetting siRNA. Significant differences between sample groups were assessed by one-way analysis of variance followed by the Bonferroni post hoc test for multiple comparisons or a two-tailed Students *t*-test was performed for single comparisons.

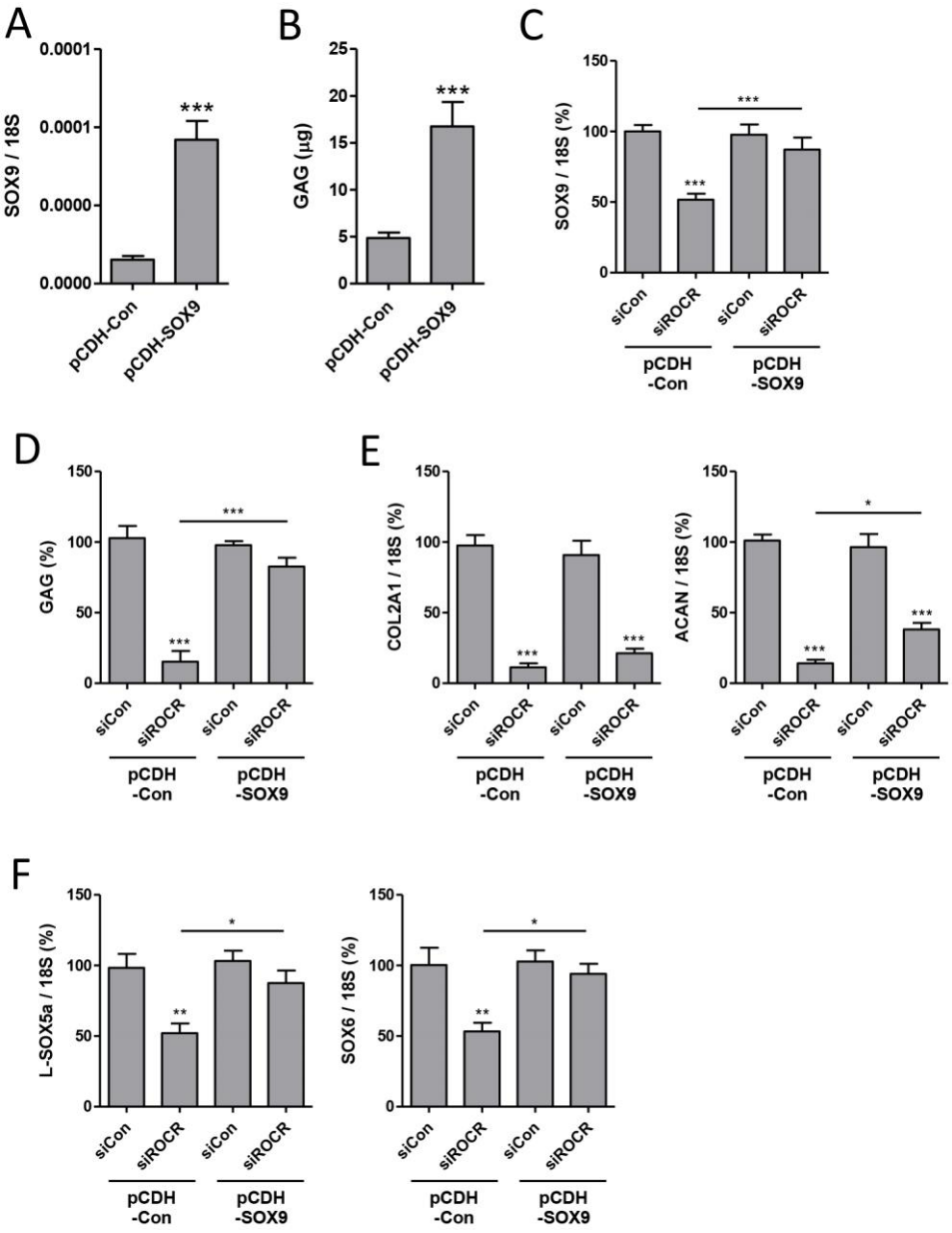

Figure 6. Effect of SOX9 overexpression in combination with *ROCR* depletion on MSC chondrogenic differentiation and gene expression

MSCs were transduced with SOX9 or control lentivirus (pCDH) for 1 day then transfected for 1 day with *ROCR*-targetting or non-targetting control siRNA prior to chondrogenic differentiation in a V-bottom 96 well plate. A. Expression of *SOX9* in only non-targetting control siRNA pellets at Day 3. B. GAG levels assayed by DMB assay in only non-targetting control siRNA pellets at Day 7. C. Expression of *SOX9* at Day 3. D. GAG levels assayed by DMB assay at Day 7. E-F. Expression of the indicated genes at Day 3. C-F. Expression is presented as a percentage of non-targetting control levels for cells transduced with each virus. Values are the mean ± SEM of data pooled from 4 MSC donors. ∗ = $P < 0.05$; ∗∗ = $P < 0.01$; ∗∗∗ = $P < 0.001$ for lncRNA siRNA versus non-targetting siRNA, or for SOX9 versus

control lentivirus where indicated above the chart. Significant differences between sample groups were assessed by one-way analysis of variance followed by the Bonferroni post hoc test for multiple comparisons or a two-tailed Students *t*-test was performed for single comparisons.

Supplementary Figure 1

A.

>*ROCR* transcript variant 1 (*LOC102723505, ENST00000430908, AC005152.3*)

AGCCTTTTAAGACACATGTTTTGGAATACAGTCAAATGCGTGCTGCTGTATGACCAGCCTATTTGAACTA
CTTAAGCATCAACTAATTAATCTGCAAGTGAAGAATACTTCCAGCATTACTCTATAATTAGACAATCTCAG
GAGGAAACAAGAGGATTTCAAAGGGGAGTCAGATGGTTTCGCAGACCGCTACATCATTTATTTTTTCATC
ACTCAGATTATGCCTCCAAATCCTACAGAAGTATAACAACCATAGAACAGACAAACACCAACAGCATCAA
CAACAGAGAAACTCAGTCCAGGAGGATATGAAACCCTTTGTAATAAAGAAAGCAACATCCATGAA

>*ROCR* transcript variant 2

AGTCCTTGAGGGACAAGAAAGTGGAGCCCAGGACTTTCCAGTCCCCACCTAGTGATCAACGTCTCACCC
ACGGTCAGGGGAGCAACTGGTGGTTCTACTTTTTTGAATTCTGAAGGCAAAGGCAAGCTTTTTTTAGGG
GTCCTGCTGTTGGCAGAGAAAGCTCCCAAGAGTTCTGCAGAGAAGAAGGATATAGACTCCAAAATTTTA
CTTCCAGGGACCATTTCAGTAGAGCCTTTTAAGACACATGTTTTGGAATACAGTCAAATGCGTGCTGCTG
TATGACCAGCCTATTTGAACTACTTAAGCATCAACTAATTAATCTGCAAGTGAAGAATACTTCCAGCATTA
CTCTATAATTAGACAATCTCAGGAGGAAACAAGAGGATTTCAAAGGGGAGTCAGATGGTTTCGCAGACC
GCTACATCATTTATTTTTTCATCACTCAGATTATGCCTCCAAATCCTACAGAAGTATAACAACCATAGAAC
AGACAAACACCAACAGCATCAACAACAGAGAAACTCAGTCCAGGAGGATATGAAACCCTTTGTAATAAA
GAAAGCAACATCCATGA

>*ROCR* transcript variant 3

CAGCGGTTGATTGCGAGGAGCAGCGGAAGGAAGGATGTATCAAACCGAAAGAAGAAAGAACCCCTGC
CAGTCGCCCCCATGACATCCGACTCTGAACGGCAGCGATCTAGAGGCTGCGGCGTGTTGCAGATTAACA
GCAGCGAGGGCAGGAGGCAAATCAGATGCCGCAGGAGCTGACTGTTTTCTTTAGCCCTGAGAGCTGAC
TGTAGGCACAGGTTGCATATCAAAGGCAACGGGAATCAGTCTGTGGCAATATTACATCAGGGACCATTT
CAGTAGAGCCTTTTAAGACACATGTTTTGGAATACAGTCAAATGCGTGCTGCTGTATGACCAGCCTATTT
GAACTACTTAAGCATCAACTAATTAATCTGCAAGTGAAGAATACTTCCAGCATTACTCTATAATTAGACAA
TCTCAGGAGGAAACAAGAGGATTTCAAAGGGGAGTCAGATGGTTTCGCAGACCGCTACATCATTTATTT
TTTCATCACTCAGATTATGCCTCCAAATCCTACAGAAGTATAACAACCATAGAACAGACAAACACCAACA
GCATCAACAACAGAGAAACTCAGTCCAGGAGGATATGAAACCCTTTGTAATAAAGAAAGCAACATCCAT
GA

B.

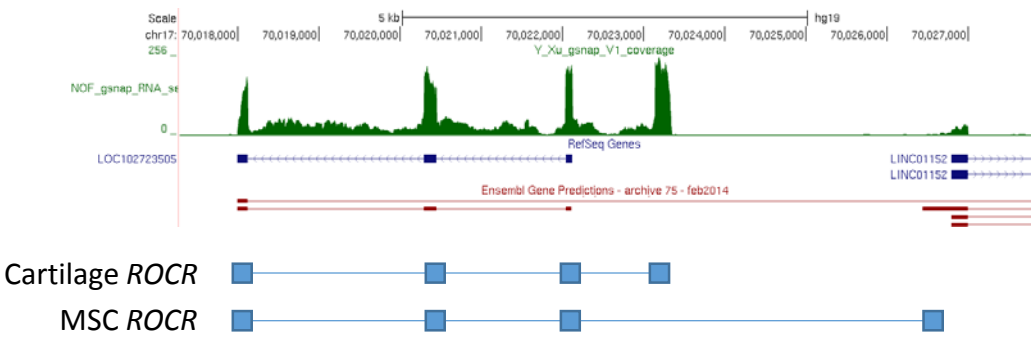

Supplementary Figure 1.

A. Transcript sequences of *ROCR* variants identified by RNA-Seq and RACE. Exons are delineated by the change between black and grey nucleotides. Primer locations are indicated by underlining (blue for exon1-2 assay, red for exon2-3 assay). B. Genome browser schematic of the two 4 exon transcript variants of *ROCR* with alternative first exons as indicated by 5'RACE from cartilage and MSC RNA.

Supplementary Figure 2

A.

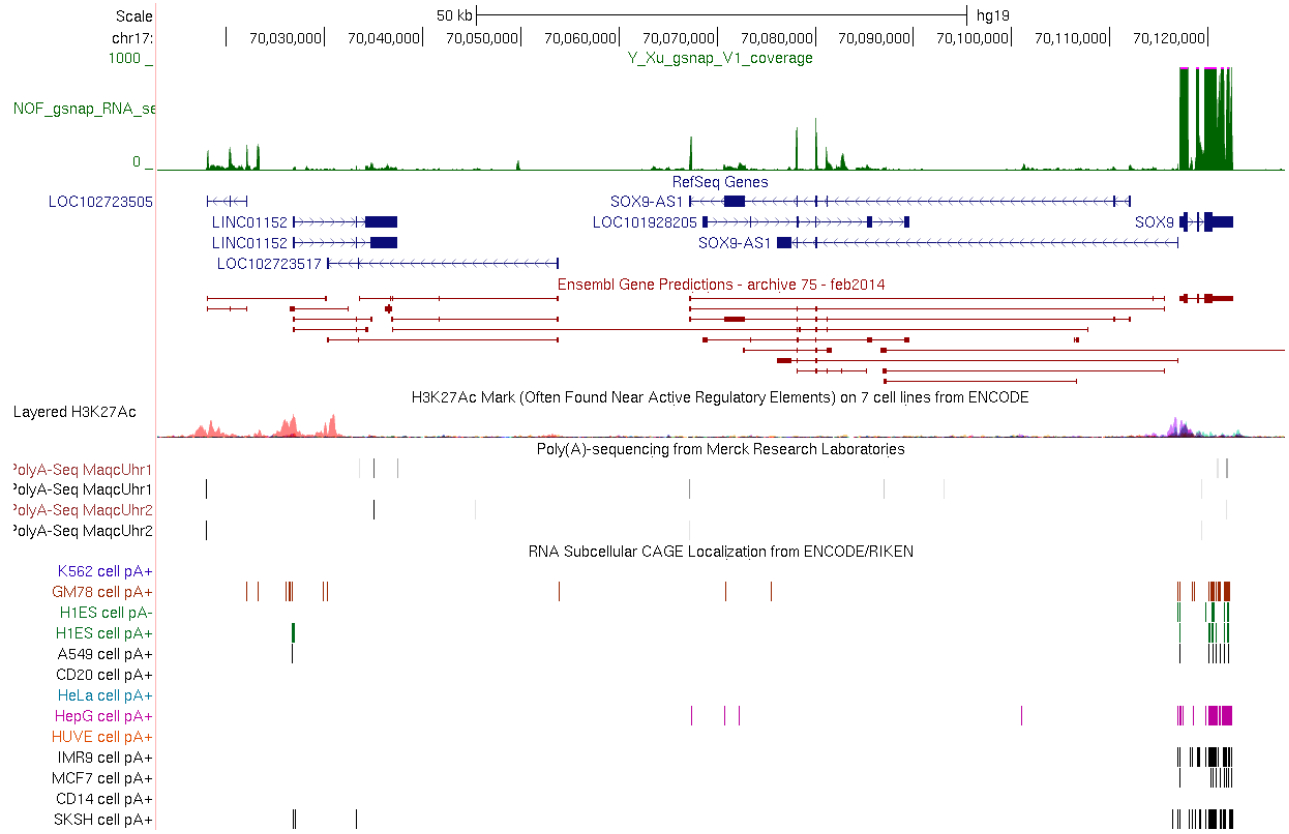

B.

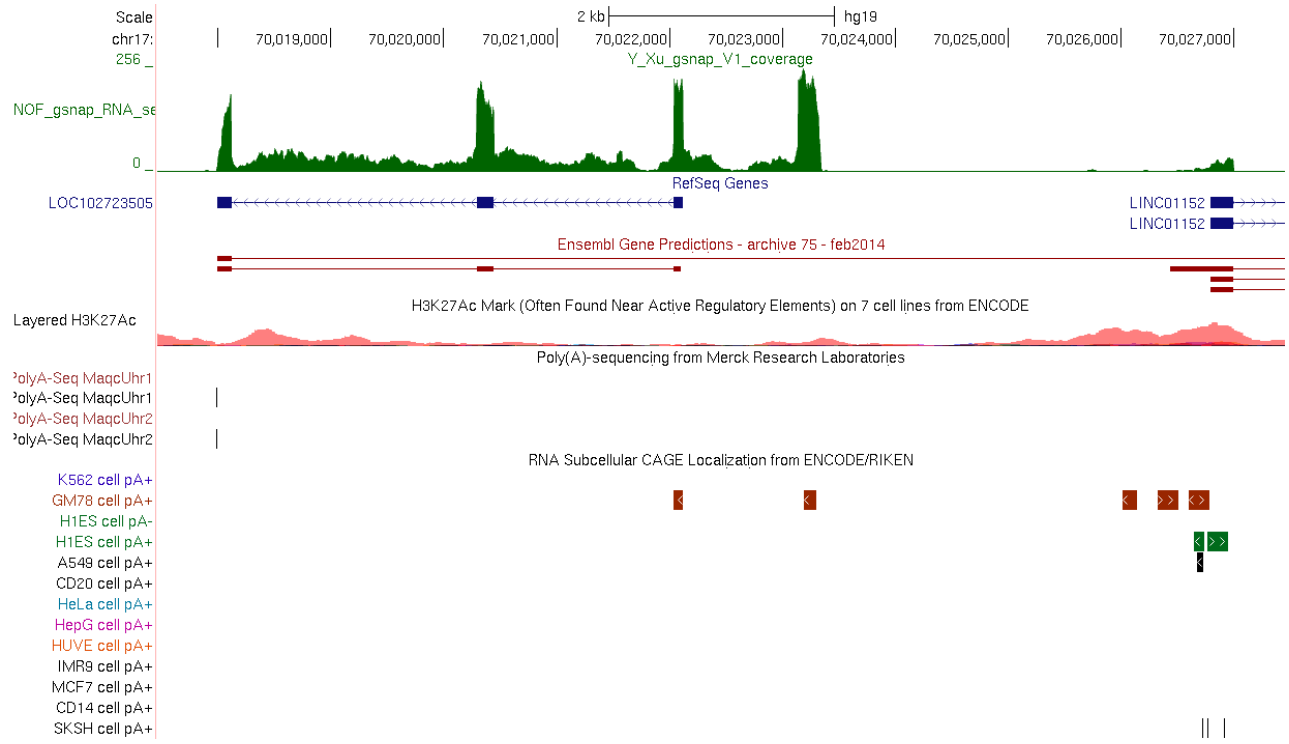

Supplementary Figure 2.

UCSC genome browser schematic of cartilage RNA-Seq reads aligned to the human genome with evidence of transcript start and end sites using CAGE (cap analysis gene expression) and PolyA-Seq data. A. *SOX9* and upstream locus. B. *ROCR* locus.

Supplementary Figure 3

A.

	ORFfinder		
	Start	**Stop**	**Length (nt | aa)**
ENST00004309 08	50	127	78 | 25
ROCR_HAC	279	356	78 | 25
ROCR_MSC	79	177	99 | 32
	329	406	78 | 25
SOX9-AS1	483	776	294 | 97
	2739	2930	192 | 63
	837	1001	165 | 54
	1511	1672	162 | 53
	125	280	156 | 51
	1393	1521	129 | 42
	76	201	126 | 41
	2295	2408	114 | 37
	2100	2204	105 | 34
	2137	2238	102 | 33
	256	351	96 | 31
	1908	1988	81 | 26
	589	666	78 | 25
LINC01152	2605	2757	153 | 50
	2571	2711	141 | 46
	1048	1179	132 | 43
	1182	1304	123 | 40
	1967	2086	120 | 39
	320	430	111 | 36
	286	390	105 | 34
	2460	2546	87 | 28
	861	944	84 | 27
	2251	2334	84 | 27
	1124	1201	78 | 25
	2803	2880	78 | 25
SOX9	373	1902	1530 | 509
	1241	1519	279 | 92
	3334	3564	231 | 76
	2668	2862	195 | 64
	2161	2322	162 | 53
	2859	2996	138 | 45
	2099	2227	129 | 42
	1927	2049	123 | 40
	2936	3037	102 | 33
	3256	3333	78 | 25

B.

		CPAT				CPC	
Sequence Name	**RNA Size**	**Fickett Score**	**Hexamer Score**	**Coding Probability**	**Coding Label**	**CODING POTENTIAL SCORE**	**C/NC**
ENST00000430908	346	0.7649	-0.081	0.012	no	-1.285	noncoding
ROCR_HAC	574	0.7649	-0.081	0.012	no	-0.758	noncoding (weak)
ROCR_MSC	624	0.7649	-0.081	0.012	no	-1.332	noncoding
SOX9-AS1	3032	1.0343	-0.010	0.128	no	-1.018	noncoding
LINC01152	3578	0.9027	-0.053	0.015	no	0.364	coding (weak)
SOX9	3963	1.3018	0.647	1.000	yes	8.199	coding

Supplementary Figure 3

C.

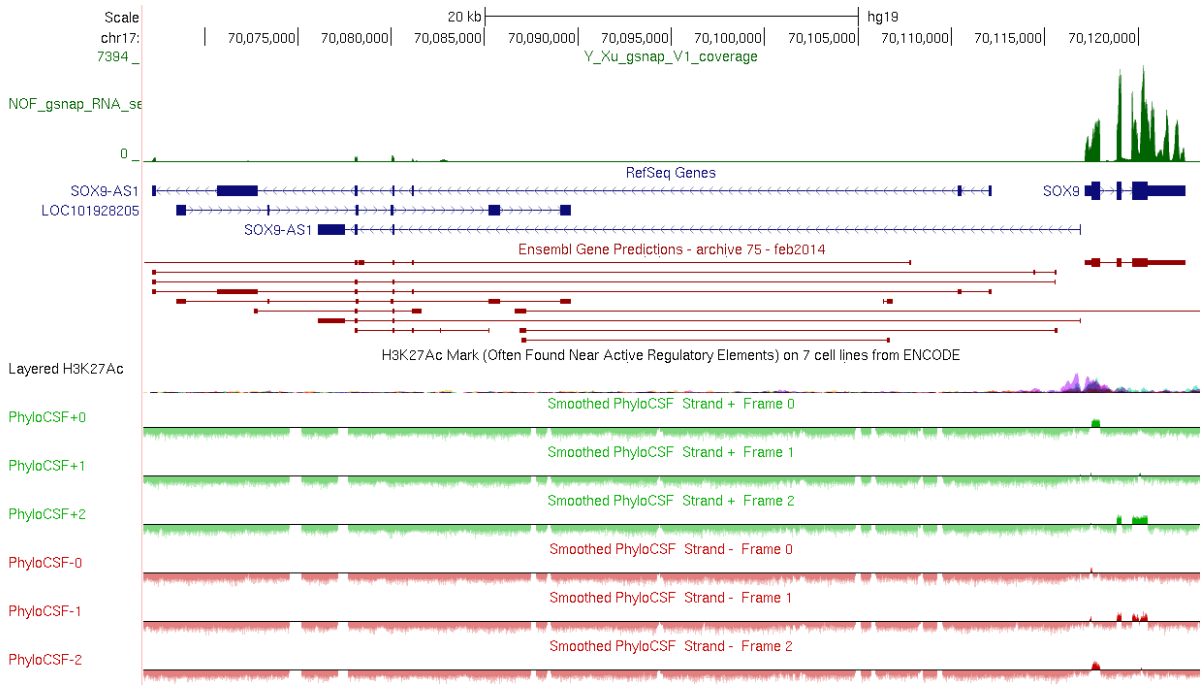

D.

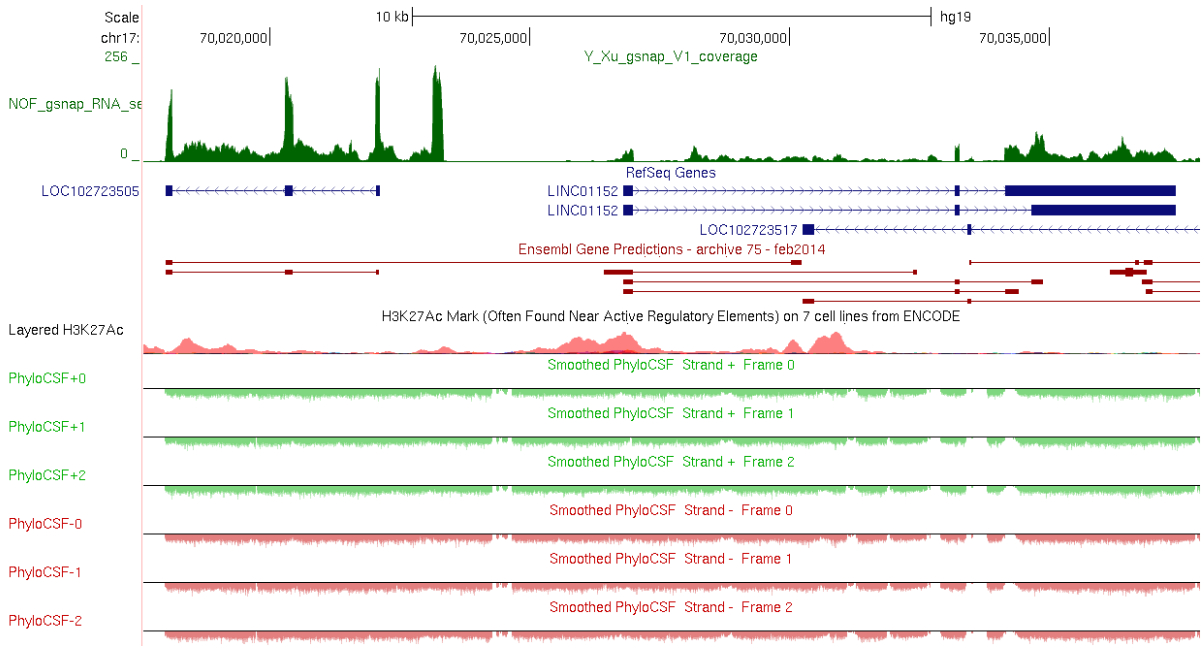

Supplementary Figure 3.

In silico analysis indicates a lack of coding potential for both *SOX9-AS1* and *ROCR*, with the existence of A. only very short open reading frames (ORF Finder) and B-D. codon substitution rates indicative of noncoding transcripts. B. CPAT and CPC. C. PhyloCSF on *SOX9* and *SOX9-AS1* locus. D. PhyloCSF on *ROCR* locus.

Supplementary Figure 4

A.

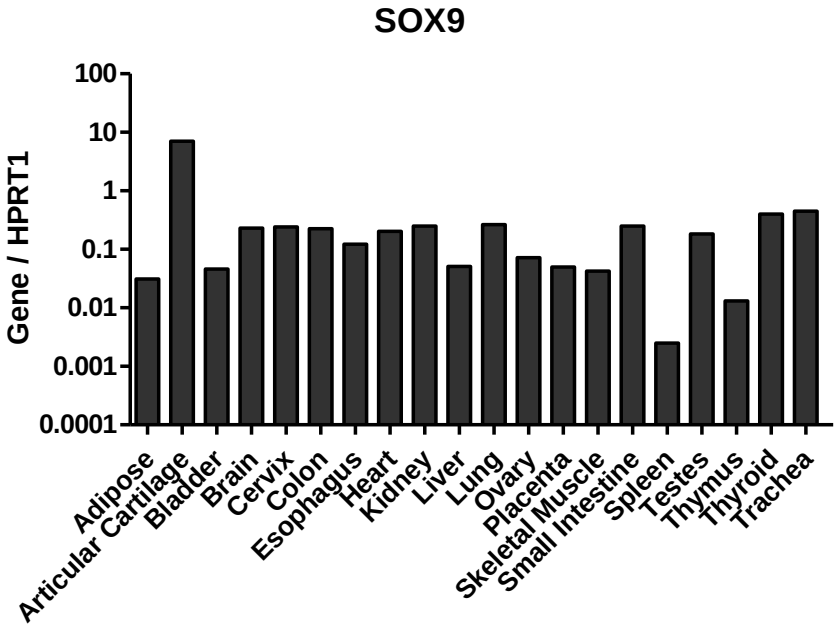

B.

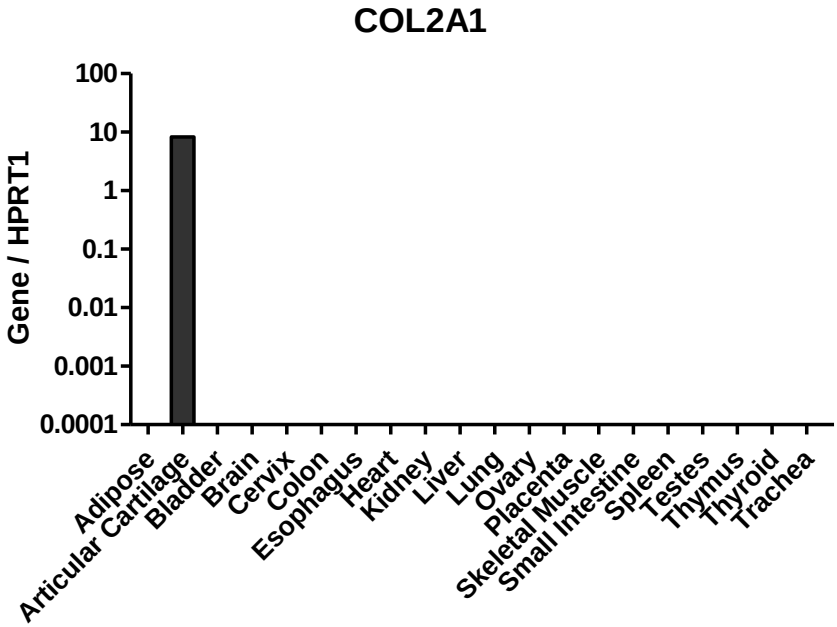

C.

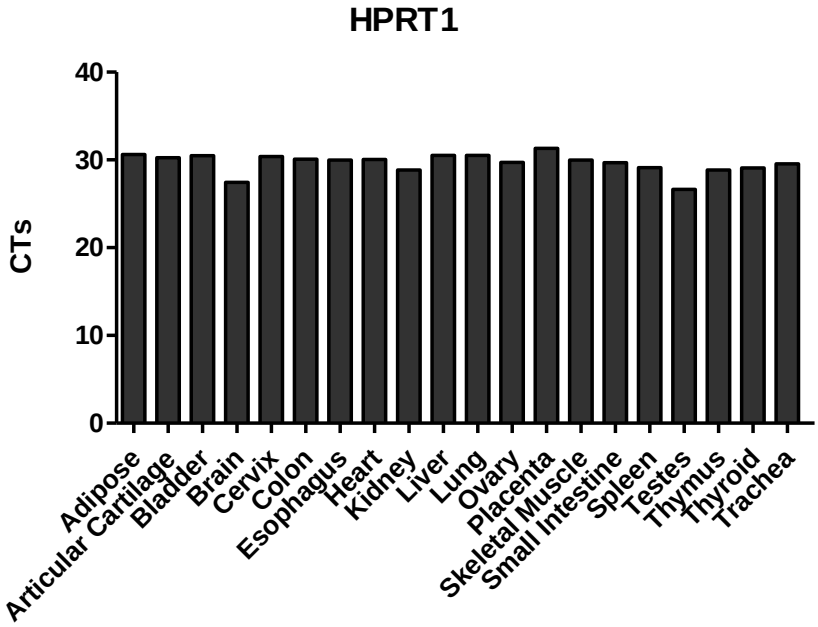

Supplementary Figure 4.

Expression of A. *SOX9*, B. *COL2A1* and C. *HPRT1* in an RNA tissue panel measured by real-time RT-PCR. Values are the technical mean of data pooled from 3 donors per tissue.

Supplementary Figure 5

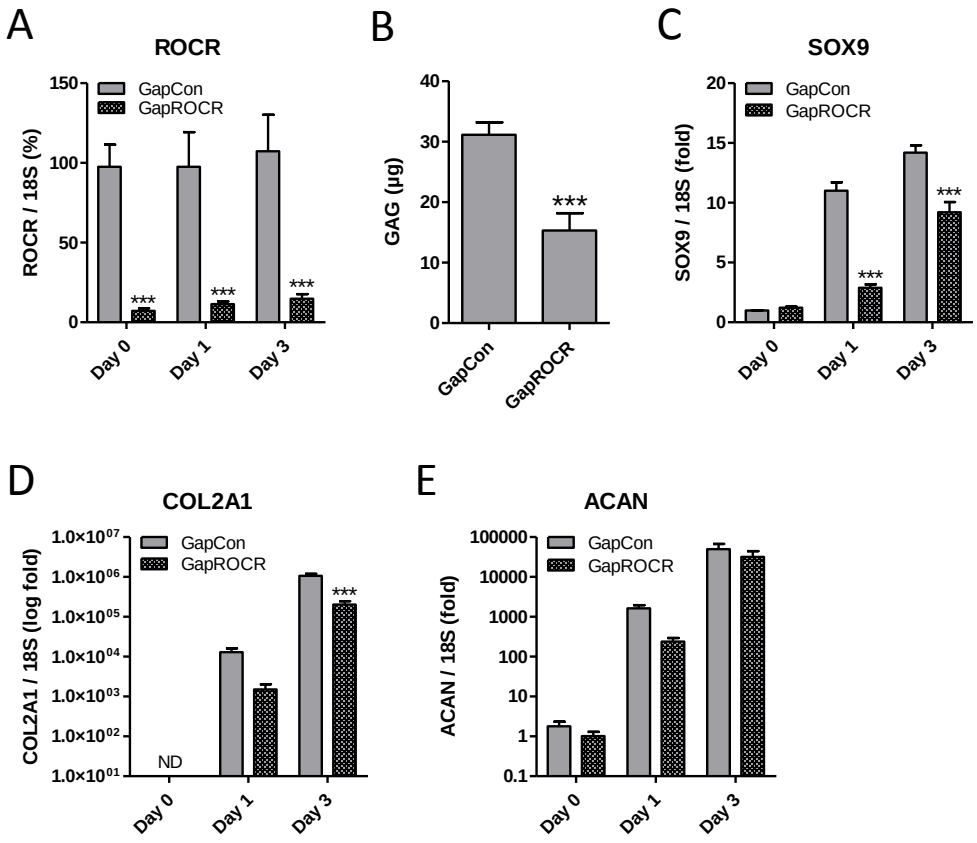

Supplementary Figure 5.

MSCs were transfected for 1 day with *ROCR*-targetting or non-targetting control GapmeR prior to chondrogenic differentiation in a V-bottom 96 well plate. A. *ROCR* expression in RNA extracted from Day 0, 1 and 3 chondrogenic pellets. Expression is presented as a percentage of non-targetting control levels. B. GAG levels assayed by DMB assay in Day 7 chondrogenic pellets. C-E. Expression of (C) *SOX9*, (D) *COL2A1*, (E) *ACAN* in RNA extracted from Day 0, 1 and 3 chondrogenic pellets. Values are the mean ± SEM of data pooled from 4 MSC donors. *** = P < 0.001 for *ROCR* GapmeR versus non-targetting GapmeR.

Supplementary Figure 6

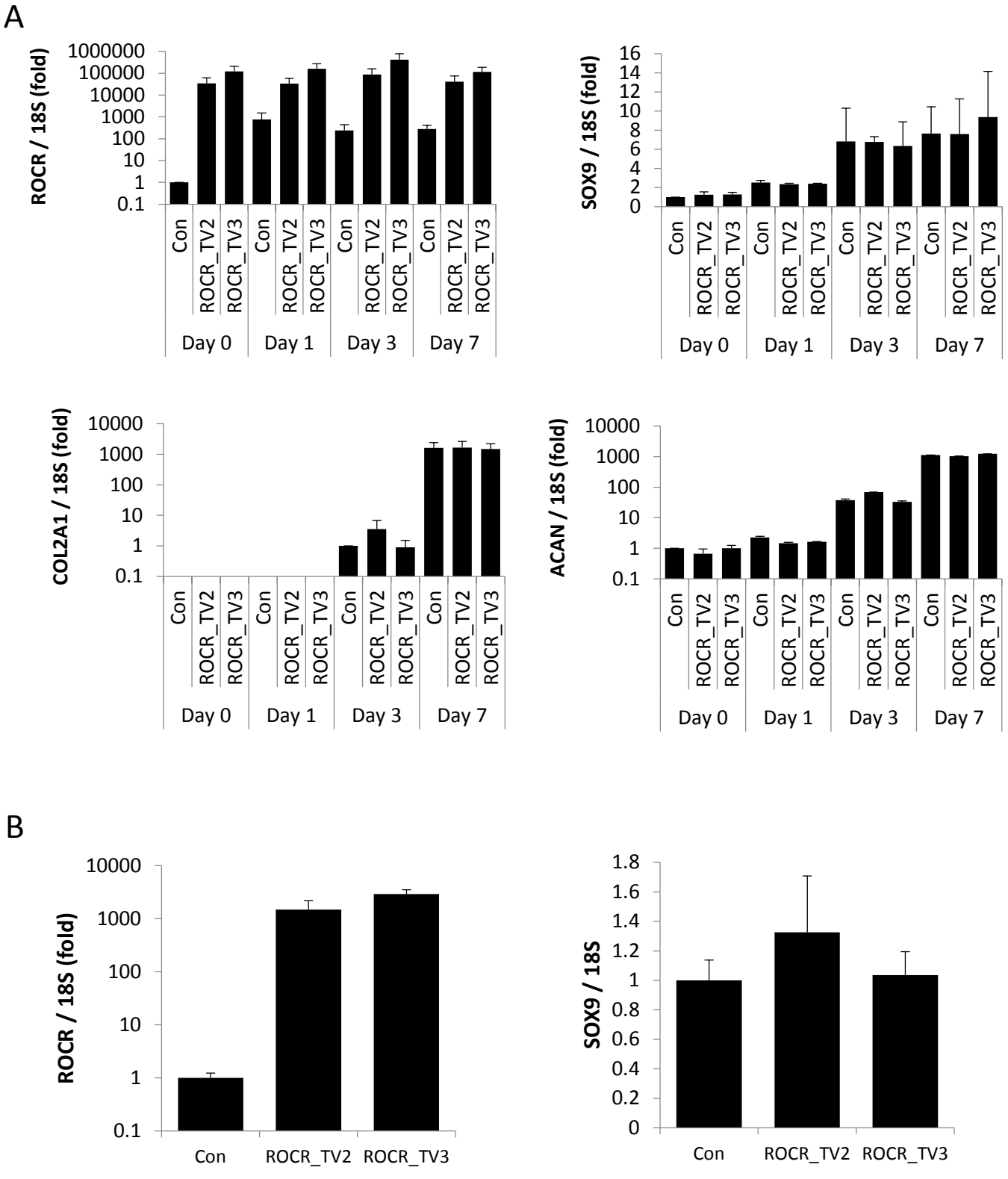

Supplementary Figure 6.

A. MSC were transduced for 2 days with *ROCR*-expressing lentivirus particles (transcript variant 2 and 3) prior to chondrogenic differentiation for up to 7 days. Expression of *ROCR*, *SOX9*, *COL2A1* and *ACAN* in RNA extracted from Day 0, 1, 3 and 7 chondrogenic pellets. Values are the mean ± SEM of data pooled from 2 MSC donors. B. *ROCR* and *SOX9* expression in HAC transduced with *ROCR*-expressing lentivirus particles (transcript variant 2 and 3) for 3 days. Values are the mean ± SEM of data pooled from 2 OA HAC donors.

Supplementary Figure 7

A.

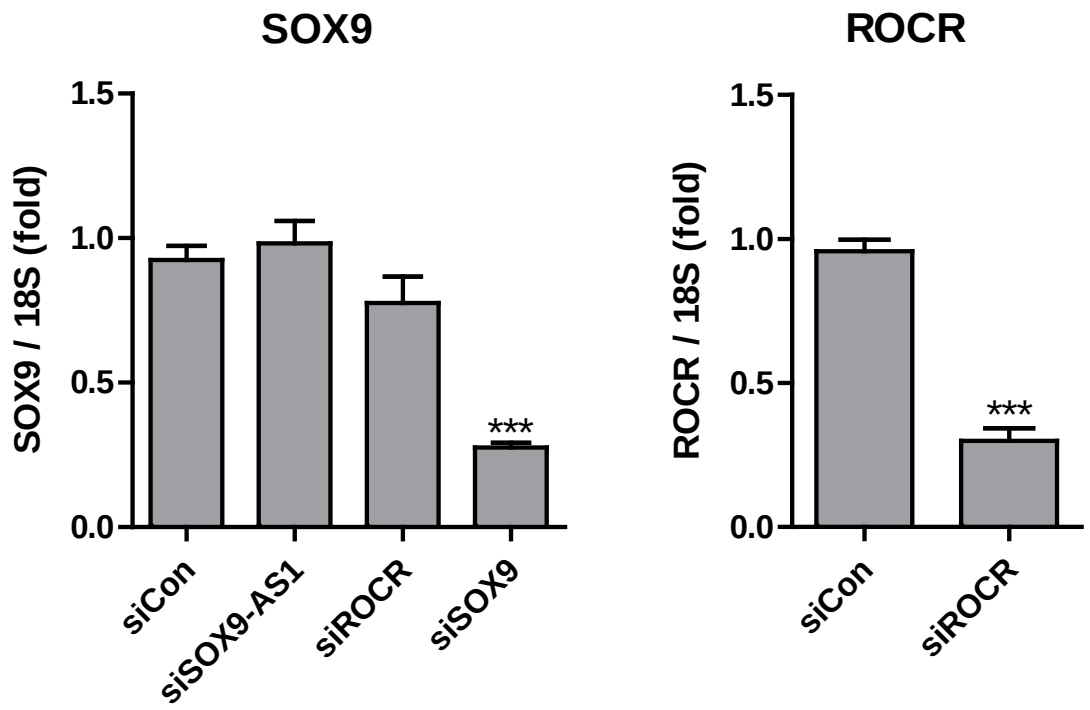

B.

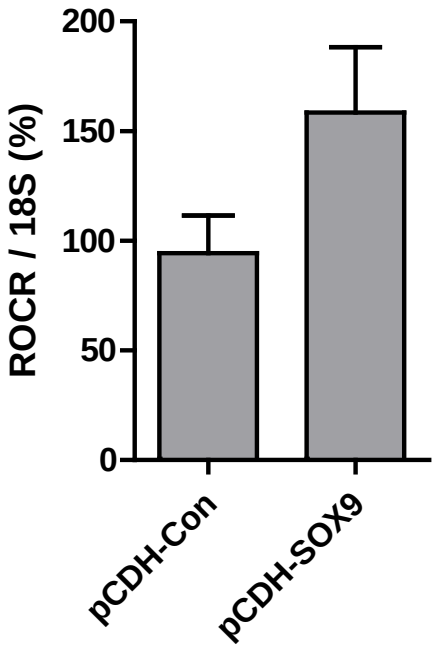

Supplementary Figure 7.

A. *SOX9* and *ROCR* expression in HAC transfected for 2 days with the indicated siRNAs. Values are the mean ± SEM of data pooled from 4 OA HAC donors. *** = P < 0.001. B. *ROCR* expression in MSCs transduced with SOX9 or control lentivirus (pCDH) for 2 days. Values are the mean ± SEM of data pooled from 4 MSC donors.

Supplementary Figure 8

A.

Mus musculus cDNA sequence BC006965 (BC006965), long non-coding RNA
Sequence ID: NR_024085.1 Length: 1952 Number of Matches: 1

Range 1: 644 to 735 GenBank Graphics Next Match Previous Match

Score	Expect	Identities	Gaps	Strand
50.0 bits(54)	9e-04	66/92(72%)	0/92(0%)	Plus/Plus

```
Query  65   GAACTACTTAAGCATCAACTAATTAATCTGCAAGTGAAGAATACTTCCAGCATTACTCTA  124
            ||||| | | |||||| ||||||||||     ||  |||||| || ||  |||  ||| |
Sbjct  644  GAACTGCGTCAGCATCCACTAATTAATCCATCAGCAAAGAATGCTGCCTCCATCTCTCCA  703

Query  125  TAATTAGACAATCTCAGGAGGAAACAAGAGGA  156
             | ||||| || |||     | ||| ||||||||
Sbjct  704  TCATTAGCCAGTCTTCAAAAGAAGCAAGAGGA  735
```

C.

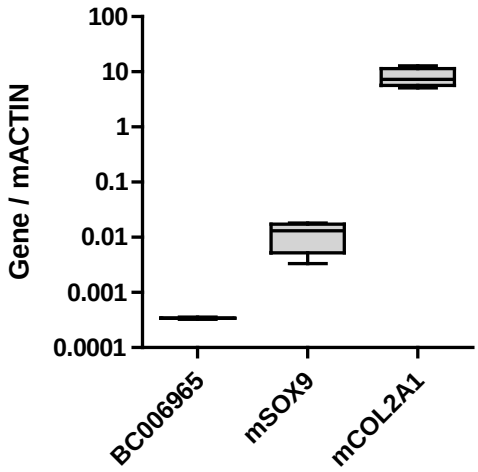

B.

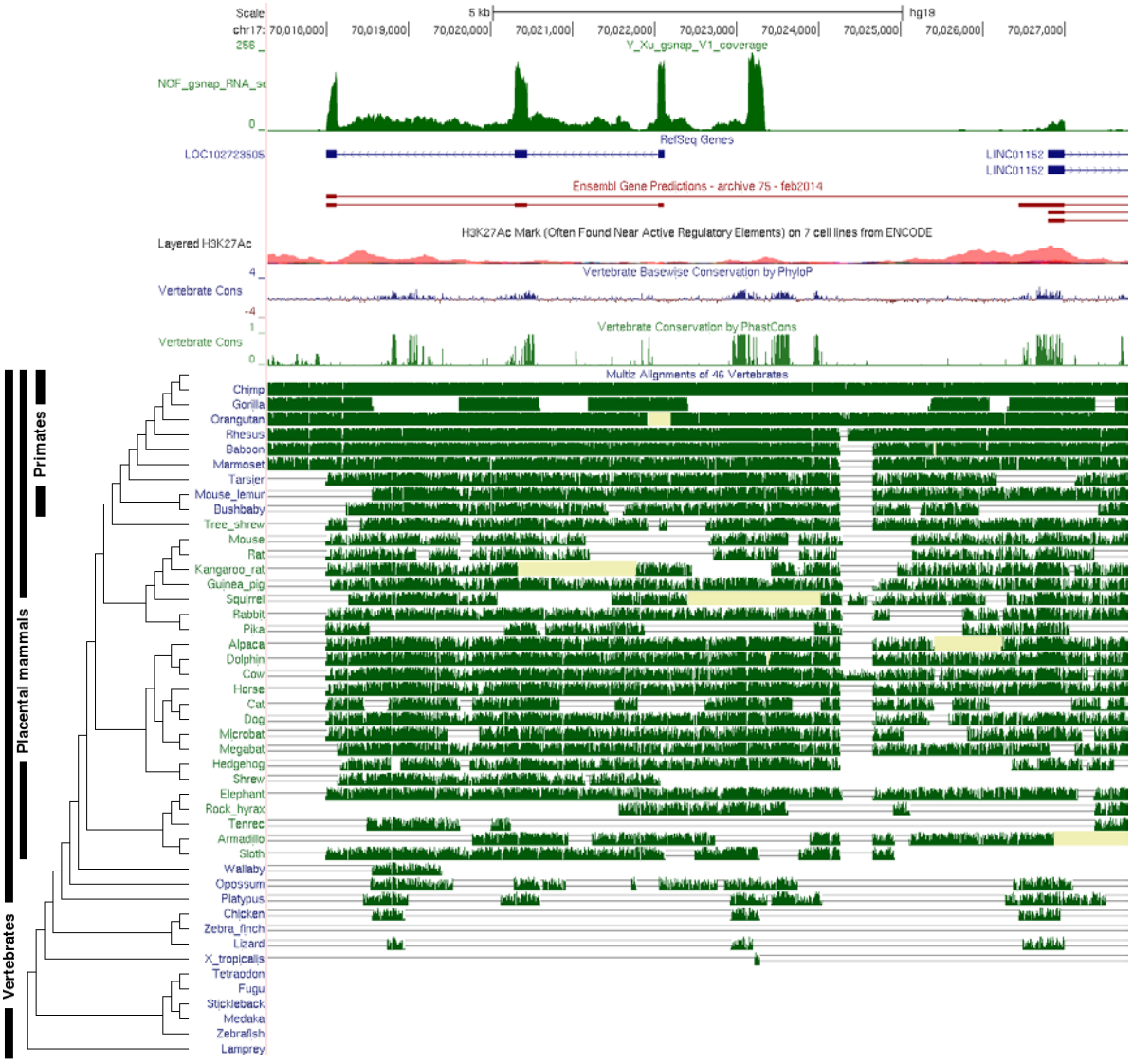

Supplementary Figure 8.

A. Blastn result of homology search for *ROCR* sequence in mouse. B. UCSC genome browser schematic of the *ROCR* locus showing vertebrate conservation. C. Expression of *Bc006965*, *Sox9* and *Col2a1* in C57BL/6 mouse xiphoid cartilage RNA.

Supplementary Figure 9

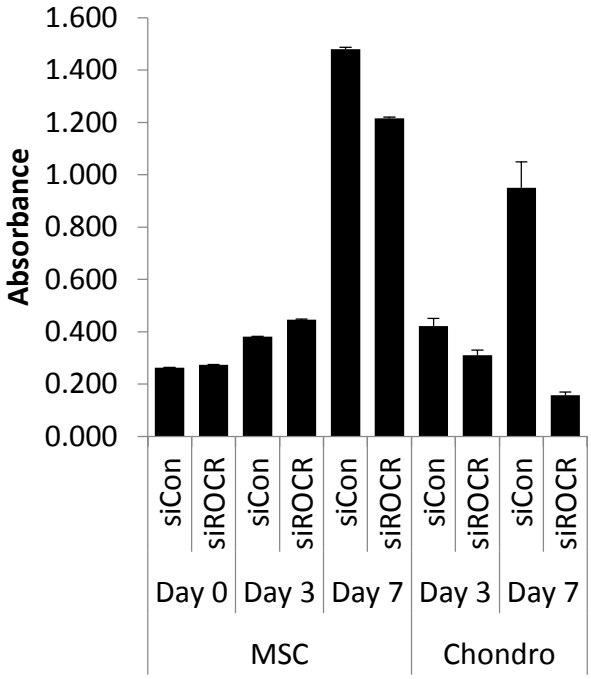

Supplementary Figure 9.

MSCs were transfected for 2 days with *ROCR*-targetting or non-targetting control siRNA prior to chondrogenic differentiation in a V-bottom 96 well plate or maintenance in MSC medium for up to 7 days. Media were collected immediately prior to the induction of chondrogenesis (Day 0) and after 3 and 7 days. Cytotoxicity was measured with the use of the Promega CytoTox 96 kit.

Supplementary Table 1.

Primer and siRNA/GapmeR sequences.

Primer	Sequence	Probe
SOX9-AS1 exon4-5 F	ccatgagcatttctcgtctg	65
SOX9-AS1 exon4-5 R	caggacaaggtggatgaaca	
SOX9-AS1 exon5-6 F	ctggcaagaggcaggaaa	38
SOX9-AS1 exon5-6 R	gctctcatccaaggtgaacag	
ROCR exon2-3 F	tgctgtatgaccagcctatttg	11
ROCR exon2-3 R	tcctcttgtttcctcctgaga	
ROCR exon1-2 F	ctgaaggcaaaggcaagc	18
ROCR exon1-2 R	caaaacatgtgtcttaaaaggctct	
LINC01152 F	cctcacttcctcctcttcctg	19
LINC01152 R	ccccatctcatctgtttttga	
RUNX2 F	gtgcctaggcgcatttca	29
RUNX2 R	gctcttcttactgagagtggaagg	
ALPL F	agaaccccaaaggcttcttc	31
ALPL R	cttggcttttccttcatggt	
ADIPOQ F	ggtgagaagggtgagaaagga	85
ADIPOQ R	tttcaccgatgtctcccttag	
FABP4 F	ccaccataaagagaaaacgagag	31
FABP4 R	gtggaagtgacgcctttcat	
L-SOX5a F	tttacctcaggagtttgaaagga	38
L-SOX5a R	gcttgtcaccatggctacct	
SOX6 F	gcttctggactcagcccttta	67
SOX6 R	ggccctttagcctttggtta	

ROCR RACE GSP1	TTTGAAATCCTCTTGTTTC
ROCR RACE GSP2	CAAAACATGTGTCTTAAAAGGCTCT

siRNA	Target sequence
siSOX9-AS1	CAAAGGAGCTAAAGAAGAA
siROCR-1	GGAGGAAACAAGAGGATTT
siROCR-2	CAACCATAGAACAGACAAA

GapmeR	Target sequence
GapROCR	ACTTAAGCATCAACTA

Supplementary Table 2.

Cartilage RNA-Seq lncRNA expression and *SOX9* expression.

Click here to Download Table S2

Supplementary Table 3.

Expression of *ROCR* and *SOX9-AS1* in cell types from Human Protein Atlas and Illumina BodyMap RNA-Seq data.

Click here to Download Table S3